Multistage Stochastic Demand-side Management for Price-Making Major Consumers of Electricity in a Co-optimized Energy and Reserve Market

Mahbubeh Habibian* †
Anthony Downward †
Golbon Zakeri †

Abstract

In this paper we take an optimization driven heuristic approach, motivated by dynamic programming, to solve a multistage stochastic optimization of energy consumption for a large manufacturer who is a price-making major consumer of electricity. We introduce a mixed-integer program that co-optimizes consumption bids and interruptible load reserve offers, for such a major consumer over a finite time horizon. By utilizing Lagrangian methods, we decompose our model through approximately pricing the constraints that link the stages together. We construct look-up tables in the form of consumption-utility curves, and use these to determine optimal consumption levels. We also present heuristics, in order to tackle the non-convexities within our model, and improve the accuracy of our policies. In the second part of the paper, we present stochastic solution methods for our model in which, we reduce the size of the scenario tree by utilizing a tailor-made scenario clustering method. Furthermore, we report on a case study that implements our models for a major consumer in the (full) New Zealand Electricity Market and present numerical results.
Keywords: OR in energy, stochastic programming, integer programming, multi-stage optimization, Lagrangian decomposition.

1 Introduction

Modelling and optimizing the production resources and processes for large manufacturers dates back to the industrial revolution. There exists a wide range of research on manufacturing

*Corresponding Author. Email: mhab735@aucklanduni.ac.nz.
†Department of Engineering Science, University of Auckland. Level 3, 70 Symonds Street, Auckland, New Zealand, 1010

optimization models, that mostly aim to minimize the cost of production, or achieve an adequate performance based on different criteria [6]. Energy consumption management is one of the major elements in controlling production resources. Among all of the different forms of energy for industrial use, electricity is different, primarily because it cannot be stored easily. Moreover, in a lot of countries, electricity is traded via a unique platform, wholesale electricity market, which is prone to high fluctuations of price, even within small time-periods. As a result, most consumers purchase electricity from retailers, or engage in medium-term contracts, with known, but higher price rates. However, for firms whose share of electricity consumption is relatively large, the difference in total energy costs is high enough to incentivize purchasing electricity directly from the wholesale market, and managing the risk of high prices through signing side-contracts, and/or demand response.

Manufacturing scheduling models that take into account electric power cost savings have recently been the focus of many studies, in various forms. These studies attempt to lay out energy-aware scheduling systems that are optimized over their specified time-horizon. For instance, in [16], an ant colony optimization is developed which considers production efficiency while taking into account the electricity consumption costs, with time-of-use pricing schemes. Mitra et al. in [18], provide deterministic optimal production planning for continuous power-intensive processes, with time-sensitive energy prices. In [25], Sun and Li utilize Markov Decision Processes (MDP) to model real-time electricity demand response for a sustainable manufacturing system, where the manufacturer curtails load, in response to unforeseen events in the market that may cause price spikes. Also, in [15], an MDP approach has been adopted to tackle the manufacturer's demand response problem, but in contrast to [25], instead of assuming a deterministic sequence of future prices, their model works with a distribution of future prices.

In electricity markets MDPs have been used to lay out dynamic demand scheduling methods. For instance in [9, 17, 19] MDP methods are used to approach price-responsive residential electricity consumption models. Moreover, in [15] a more general MDP approach is used to present a demand-response method for non-interruptible and interruptible loads.

In all the papers mentioned above and the similar existing literature on manufacturer's demand response, electricity price is given as an exogenous parameter. However, the assumption of price-taking consumers is, in many cases, an over-simplification. The most significant difference in studying large manufacturers' demand response, as opposed to studying optimized price-responsive demand policies for residential consumers [21, 27], lies in the acknowledgment of the impacts of the large agent's actions on the spot prices. Often, large manufacturers have sizable-enough loads that changing their consumption could have a significant impact on the electricity

price; it is important that this ability to affect the price is represented in the mathematical modeling of such problems.

Due to the "hockey stick" nature of electricity stacks (as we approach system capacity the prices rise sharply), cutting down the consumption during high price periods not only reduces the purchase of high priced electricity, but also leads to a decrease in spot prices, and a resulting reduction in the total energy costs of the manufacturing processes. Promoting flexibility in electricity consumption also enables these firms to participate in the reserve market and gain extra revenue through providing ancillary services. In addition, offering interruptible load reserve (ILR) allows the consumers to alleviate any pressure on reserve that may in turn affect the price of electricity.

In this paper we focus on large manufacturers who purchase electricity from a co-optimized energy and reserve market, such as New Zealand or Singapore, while taking into account the influence of their actions on the prices of energy and reserve. In co-optimized markets each major consumer can submit an ILR offer alongside their consumption bid for each trading period. Therefore, in this paper we study demand response for price-making major consumers, in order to develop a realistic multistage stochastic load scheduling for such manufacturers. We will use the New Zealand Electricity Market (NZEM) data to build a realistic full-scale model.

In New Zealand, almost all manufacturers are large consumers of electricity, and many of these manufacturers are capable of interrupting their manufacturing process, at least for a short while. Pulp and paper mills and steel manufacturers are examples of manufacturers with some flexibility for interruption of their electricity supply. Aluminium smelters have been regarded as inflexible. However a new technology has been developed for the New Zealand Aluminium Smelter (NZAS), which makes the smelter capable of demand response by allowing the cells to dispense with electrical current running through them without the cell "freezing" [26]. The NZAS load is in particular, has a large impact on the NZEM, as it consumes approximately 15% of the volume of electricity purchased in New Zealand. Therefore, we have used this firm's historical data in our case studies to benchmark the effectiveness of our proposed policies.

Responding to price can reduce the cost for the consumers. However, there is a limit on how much flexibility a manufacturer has in changing its production plan. Most of these major consumers have contracts that obligate them to produce certain quantities within a given time period. In order to present a realistic consumption plan for such manufacturers we incorporate a total consumption requirement over a finite time horizon. This allows for load shifting between stages, while maintaining the production requirements over the specified time horizon. However,

adding this constraint will make the optimization problem hard to solve, since the stages will become linked together.

Our aim is to solve this multistage optimization problem for a month-long time horizon. Given each day consists of 48 time-periods, the number of stages for this optimization problem is 1440. Solving such optimization problem becomes more challenging when uncertainty is introduced to the model, and we need to maximize the expected profit over such a time horizon. Our approach in this paper is to use Lagrangian decomposition techniques to tackle the complexity of the problem, by taking into account the structure of the problem. The closest work that has been done on this problem is by Steeger et al. in [23, 24], where they address a price-maker hydro-electric generator who strategically offers energy over a time-horizon. The method that they use to tackle the integrality of the value function is to convexify the future expected value curves, which is an approximation of the true value functions. Our method, however, tackles non-convexities through utilizing step-wise value curves with higher accuracy. In addition, in [23, 24], the solution method is applied on a 24-stage time horizon, and operates over the equivalent of a single-node network, whereas our case-study is a large real world application, consisting of 1440 stages, and a 270-node network. Therefore, in order to reduce the size of the corresponding scenario tree, we introduce a sensitivity analysis based clustering method that approximates our endogenous price process.

The paper is laid out as follows. Section 2 introduces the single-stage co-optimization for a major consumer, represented by a MIP (mixed-integer program). It is followed by Section 3, where we extend the multistage co-optimization over a finite time horizon, and by utilizing Lagrangian methods decompose the model. In Section 4 we move to optimization under uncertainty and propose a heuristic clustering method. In Section 5, we apply the stochastic optimization for a major consumer of energy in the NZEM and report on the performance of our proposed policy. Section 6 concludes the paper.

2 Co-optimization of energy and reserve

We view our consumer as a strategic, price-making agent. We start by assuming that at a given time period, this consumer maximizes its profit through deciding on its energy consumption bid and ILR offer. As the consumer is a price maker, the optimal power flow (OPF) problem is embedded within the consumer's profit optimization problem, rendering a leader-follower type model captured as a bi-level program. (See Appendix A for the detailed strategic consumer's bi-level problem.) In order to solve this mathematical program, following [8], we convert the bi-level model to a mixed-integer program (MIP), utilizing a bi-parametric sensitivity analysis

reformulation method. In this paper we present our MIP in a generic form as below:

$$\begin{aligned} [\text{MIP}]_{t,v} \quad & \max \Pi_t(\mathbf{x}_t) = vx_t - \mathcal{C}_t(\mathbf{x}_t) \\ & \text{s.t. } \mathbf{x}_t \in \mathcal{S}_t. \end{aligned}$$

Here $\mathbf{x}_t$ is a vector of decision variables at time t (in our model it consists of consumption and ILR), and x_t is the consumption level at time t. Also v is the value of consuming one unit of electricity, $\mathcal{C}_t$ is the cost function at time t, and $\mathcal{S}_t$ forms the feasible set at stage t, which may be non-convex. Note that for each time period MIP is a large optimization problem that is derived from a bi-level problem that maximizes a price-maker major consumer's profit while solving the co-optimized OPF in the lower level. In NZEM, the OPF is solved over 250 nodes.

One of the important parameters in the single-stage co-optimization is the marginal value of energy consumption. In the absence of a total consumption target, we can solve each time period separately according to the marginal value of electricity consumption. However, when there is a total consumption goal, the stages are linked together. In the next section, we extend our model over a time horizon, and present solution methods.

3 Co-optimization over a time-horizon

Optimal actions of strategic major consumers are highly influenced by the marginal value of consumption. This value is affected by various parameters such as the global price of a manufacturer's product, labour costs, etc. This utility also may change slightly or drastically throughout time for industrial consumers, due to changes in the product price or government policies. For this reason, manufacturers typically enter into long-term contracts to deliver specific quantities of their product by a given date; so the question becomes "how should a manufacturer choose to schedule consumption in order to minimize its total cost?".

Therefore, in this paper we aim to change our point-of-view from a marginal value perspective (as was the focus of [8]) to a total consumption value target, and plan consumer's load over a given time horizon. Below we lay out a model that optimizes the consumption and ILR levels for a strategic consumer, given a total consumption level G over a time horizon $\mathcal{T}$.

$$\begin{aligned} [\text{MIP}] \quad & \max \Pi(\mathbf{x}) = -\sum_{t\in\mathcal{T}} \mathcal{C}_t(\mathbf{x}_t) + \sum_{t\in\mathcal{T}} vx_t \\ & \text{s.t. } \mathbf{x}_t \in \mathcal{S}_t && \forall t \in \mathcal{T} \\ & \sum_{t\in\mathcal{T}} x_t = G. \end{aligned}$$

Here $\mathbf{x}^*$ is the optimal solution to [MIP], hence $\sum_{t\in\mathcal{T}} vx_t^* = vG$, which is a constant. This shows that the marginal value of consumption will not affect the optimal actions, since the total consumption value is the key parameter to control consumption at each time period[1]. In this model we consider this value to be exogenous to our model. Given the observation above, we continue by defining [CM-MIP]. Note that the optimal solution to [MIP] solves [CM-MIP].

$$\begin{aligned} \text{[CM-MIP]} \quad \mathcal{Z}(G) = \min \ & \sum_{t\in\mathcal{T}} \mathcal{C}_t(\mathbf{x}_t) \\ \text{s.t. } & \mathbf{x}_t \in \mathcal{S}_t && \forall t \in \mathcal{T} \\ & \sum_{t\in\mathcal{T}} x_t = G. \end{aligned}$$

In the rest of this paper we attempt to solve [CM-MIP], where each [MIP] is a complicated optimization program (see Appendix A), and over a large $\mathcal{T}$; which results in a very complex model. Given that this large problem cannot be solved with commercial solvers in a reasonable time-frame, decomposition methods are needed in order to find the optimal policy. In particular, we will implement a decomposition method which enables the flexibility to change the problem parameters (e.g. total consumption value) throughout the optimization period.

3.1 Dynamic programming

In this section, we aim to decompose our MIP in a way such that we can solve each time-period separately, while taking into account the effects of the actions in each time-period on future consumption requirements. At first glance, the structure of [MIP] fits well to be solved via dynamic programming, with the "consumption to go" as the one-dimensional state variable. However, this standard approach does not perform efficiently as the number of states becomes very large for long time-horizons. For instance, for a weekly plan, if we discretize the states by 1MW steps, while assuming that the consumer can consume up to 800MWh at each trading periods, the number of states is 268800 for each stage. Furthermore, in order to calculate the stage-cost for a given time period t, we need to solve $[\text{CM-MIP}]_t$[2]. In addition, in this approach it is necessary to discretize the consumption quantity. However, our goal is to offer a non-discretized optimal demand schedule for a major consumer, in a practical time-frame, hence we will present alternative decomposition methods.

[1]When the decision makers set the value G for their firm, they already have taken into account the average marginal value of consumption over the designated time horizon.

[2]The reason we are required to solve a MIP rather than simply solving the dispatch LP is due to the fact that the major consumer strategically offers ILR that is co-optimized with the consumption level. Please see [8] for the detailed strategic consumer's co-optimized model.

3.2 Lagrangian methods

A commonly-used approach to decompose a master-problem with a constraint that links the sub-problems together is Lagrangian relaxation. In order to decompose our model we take advantage of the unique properties of our model, in addition, we adapt ideas from decomposition methods for convex models. We start with a price-taking model (which is convex), and we will then extend this methodology and apply it to the [MIP] model.

3.2.1 Decomposition method for price-taking consumer

In this section we define an LP, where a price-taking consumer minimizes its cost, given a total consumption quantity G MWh is required, over the set of linear constraints S_t, $\forall t \in \mathcal{T}$.

$$\begin{aligned} [\text{LP}] \quad & \min \sum_{t\in\mathcal{T}} \mathcal{C}_t(\mathbf{x}_t) & \\ & \text{s.t. } \mathbf{x}_t \in S_t & \forall t \in \mathcal{T} \\ & \sum_{t\in\mathcal{T}} x_t = G & [u] \end{aligned}$$

In the next step, we use the Lagrangian relaxation method to reformulate the LP as below:

$$\begin{aligned} [\text{LP}] \quad & \min \sum_{t\in\mathcal{T}} \mathcal{C}_t(\mathbf{x}_t) - u(\sum_{t\in\mathcal{T}} x_t - G) & \\ & \text{s.t. } \mathbf{x}_t \in S_t & \forall t \in \mathcal{T} \end{aligned}$$

Given G is a constant, if we find the right $u = \hat{u}$ that solves [LP], we can separate [LP] by time periods. Hence for each $t \in \mathcal{T}$ we have:

$$\begin{aligned} [\text{LP}]_t \quad & \min \mathcal{C}_t(\mathbf{x}_t) - \hat{u}x_t \\ & \text{s.t. } \mathbf{x}_t \in S_t. \end{aligned}$$

Assuming strict convexity, $\hat{u}$ is essentially an increasing function of the consumption quantity G. The higher $\hat{u}$ is, the more the consumer will consume. In the next section, we transition to the price-maker consumer model by adapting this decomposition method for our MIP model, but as we will see, $\hat{u}$ will no longer be a function of G.

3.2.2 Price maker model

In the price-maker version, since the model is non-convex, we cannot acquire a dual variable on the total consumption constraint. However, by utilizing the idea of Lagrangian relaxation, we

can reformulate our model, using a parameter which mirrors the properties of a multiplier. In order to build a decomposed MIP, we define $[\text{U-MIP}]_u$ as the problem with the total consumption constraint removed, and instead valued in the objective. Lemma below provides a sufficient condition where the optimal solution of $[\text{U-MIP}]_u$ solves [CM-MIP].

$$\begin{aligned} [\text{U-MIP}]_u \quad \max \; & -\sum_{t\in\mathcal{T}} \mathcal{C}_t(\mathbf{x}_t) + \sum_{t\in\mathcal{T}} u x_t \\ \text{s.t. } & \mathbf{x}_t \in \mathcal{S}_t \qquad\qquad \forall t \in \mathcal{T} \end{aligned}$$

Lemma 3.1. *Let $\mathbf{x}^*$ be the optimal solution to [U-MIP]$_u$, for some $u \geq 0$. Then $\mathbf{x}^*$ solves [CM-MIP] with $G = \sum_{t\in\mathcal{T}} x_t^*$.*

Proof.

$$\begin{aligned} &\Pi(\mathbf{x}^*) = -\sum_{t\in\mathcal{T}} \mathcal{C}_t(\mathbf{x}_t^*) + \sum_{t\in\mathcal{T}} u x_t^* \geq -\sum_{t\in\mathcal{T}} \mathcal{C}_t(\hat{\mathbf{x}}_t) + \sum_{t\in\mathcal{T}} u \hat{x}_t \qquad \forall \hat{x}_t \in \mathcal{X} \\ &\Rightarrow \sum_{t\in\mathcal{T}} \mathcal{C}_t(\hat{\mathbf{x}}_t) \geq \sum_{t\in\mathcal{T}} u(\hat{x}_t - x_t^*) + \sum_{t\in\mathcal{T}} \mathcal{C}_t(\mathbf{x}_t^*) \\ &\Rightarrow \sum_{t\in\mathcal{T}} \mathcal{C}_t(\hat{\mathbf{x}}_t) \geq \sum_{t\in\mathcal{T}} \mathcal{C}_t(\mathbf{x}_t^*) \end{aligned}$$

□

Note that $[\text{U-MIP}]_u$ is decomposable to each time period (as $[\text{U-MIP}]_{t,u}$ and $[\text{MIP}]_{t,v}$[3] are the same). The next step is to find the right value of the parameter u in order to find the optimal actions, for valid given total consumption values G. In order to make policies that result in finding the right value of u, without relying on convexity, or continuity, we introduce the Utility-Consumption (U-C) curves in the next part.

3.3 Utility-consumption curves

In order to show the properties of the model with respect to the u parameter value and optimal consumption level, we construct look-up curves. The idea of using such curves is introduced in [22] for a hydro-scheduling setting, whereas in this paper we extend this concept to a price-making optimal consumption model.

[3]Note that $[\text{MIP}]_{t,v}$ from Section 2 and $[\text{U-MIP}]_{t,u}$ are essentially the same optimization problem. Recall that the interpretation of parameter v in $[\text{MIP}]_{t,v}$ is the marginal value of consuming electricity; whereas the parameter u in $[\text{U-MIP}]_{t,u}$ is the multiplier on the total consumption constraint. Hence, although we have changed our perspective from a marginal utility point of view to a Lagrange multiplier value, these two parameter are identical.

In this section, in order to construct the U-C curves for each trading period t we solve $[\text{MIP}]_{t,u}$, $\forall u \in [0, u_{\max}]$, and plot the values of u versus its optimal consumption level, $g(u,t) = x_t^*$ (shown in Figure 1). Mapping the consumption level to utility values is essentially a set valued mapping. In particular $[0, u_{\max}]$ is partitioned by a finite number of sub-intervals (indexed by k) such that $\forall u \in (u_k, u_{k+1})$, $g(u)$ is constant.

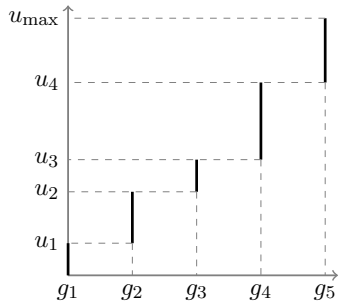

Figure 1: U-C for one TP

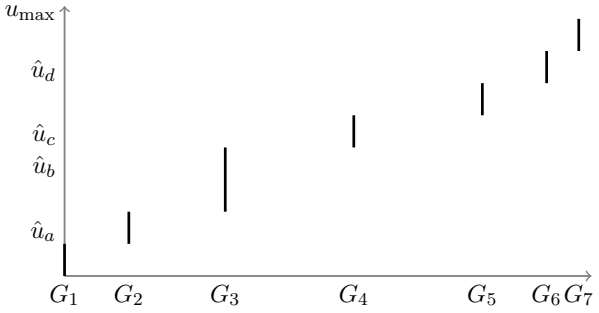

Figure 2: Aggregate U-C

As demonstrated in Figure 1 for each of the finite number of ranges of parameter u, the optimal consumption remains constant within the range. Also we observe that by increasing u, the consumption value jumps to a higher consumption level. Below we prove that the U-C curves are monotone increasing.

Lemma 3.2. *Let $\mathbf{x}^*$ be the optimal solution to $[\text{MIP}]_{t,u}$, for some t and u, and $\Pi(\mathbf{x}^*, u)$ be the optimal objective function value of $[\text{MIP}]_{t,u}$. Then $\forall u \geq 0$, $x^*(u)$ is monotone .*

Proof. We will first define $[\text{MIP}]_{t,u'}$, for some $u' > u$, where $\Pi(\mathbf{x}^{*\prime}, u')$ is the optimal objective value for $[\text{MIP}]_{t,u'}$; that is laid out below:

$$[\text{MIP}]_{t,u'} \max -\mathcal{C}(\mathbf{x}) + ux + (u' - u)x$$
$$\text{s.t. } \mathbf{x} \in \mathcal{S}.$$

Using the definition of $[\text{MIP}]_{t,u'}$ and $[\text{MIP}]_{t,u}$, we have:
$\Pi(\mathbf{x}^*, u) = \Pi(\mathbf{x}^*, u') - (u' - u)x^*$ and $\Pi(\mathbf{x}^{*\prime}, u) = \Pi(\mathbf{x}^{*\prime}, u') - (u' - u)x^{*\prime}$.
Given $\mathbf{x}^*$ is the optimal value of $\mathbf{x}$ for $[\text{MIP}]_{t,u}$, then no objective function value higher than $\Pi(\mathbf{x}^*, u)$ can be obtained for $[\text{MIP}]_{t,u}$. Therefore, we have:
$\Pi(\mathbf{x}^*, u) \geq \Pi(\mathbf{x}^{*\prime}, u) \implies \Pi(\mathbf{x}^*, u') \geq \Pi(\mathbf{x}^{*\prime}, u') - (u' - u)(x^{*\prime} - x^*)$.
Using the expression above we prove our lemma by contradiction. Suppose $x'^* < x^*$, therefore we have $(u'-u)(x^{*\prime}-x^*) < 0$, this implies $\Pi(\mathbf{x}^*, u') > \Pi(\mathbf{x}^{*\prime}, u')$ which yields a contradiction. □

In order to build U-C curves, we first define the order of G values in $\mathcal{G}$ from lowest to highest. Given the monotonicity of G with respect to u, we know that for the first G value in $\mathcal{G}$ there

will be a lower associated u value than the second G in $\mathcal{G}$; this property enables us to easily build the whole curve. The next step is to find the optimal policy, via the aggregated U-C curve over all time periods. In order to make the aggregated curve, for any value of the parameter u, we compute the the sum of corresponding optimal consumption values over all trading periods' individual U-C curves in the time horizon. Therefore for each u we have the total consumption values in the aggregated U-C curve $G(u) = \sum_{t\in\mathcal{T}} g(t,u)$. Figure 2 shows an aggregated curve where the horizontal axis corresponds to total consumption values.

Given the method used for aggregating the U-C curve, the aggregated curves will have more pieces than the sum of individual time-periods' curves. Here the points on the total consumption (G) axis, form the set of total consumption values $\mathcal{G} = \{G_1, G_2, \ldots, G_5\}$ that we can choose from. After choosing G, we can look up our U-C curve and find the range of optimal $\hat{u}$ values for our model. Therefore we can solve each $[\text{U-MIP}]_{t,\hat{u}}$ separately, given $\hat{u}$. However in the case where $\hat{G} \notin \mathcal{G}$, the optimal solution to $[\text{U-MIP}]_u$ is not equivalent to that of [CM-MIP], as there is no $u = \hat{u}$ such that $\sum_{t\in\mathcal{T}} x_t^* = \hat{G}$. Hence we cannot simply use the aggregate U-C curve to calculate the consumption in each time period.

The structure of our U-C curves indicate that to increase any designated $G \in \mathcal{G}$ value, we simply increase consumption in some trading periods, i.e. there is no decrease of consumption in any of the time-periods; this means that lower G values are nested within higher Gs. However, for $G \notin \mathcal{G}$ the nested property might not apply, and the optimal solution could indicate decreasing consumption at one trading period and increasing consumption in another. In order to address this issue we present a heuristic method and bounds on the its solution in the following sections.

3.4 Heuristics

In this section we introduce a heuristic algorithm to extract policies from the aggregate U-C curves, for any given value of G. First, for each time period's U-C curve, we connect the vertical lines with virtual horizontal lines, to make step functions. This step-wise function has the same attributes as a supply function for a generator in the dispatch model (presented in Appendix A). We view each time period as a node, and the total consumption value as the demand. We introduce [HEU], where we minimize utility $\times$ consumption.

$$
\begin{aligned}
[\text{HEU}] \quad \min \; & \sum_{t\in\mathcal{T}} \sum_{i\in\mathcal{I}_t} u_t^i x_t^i & \\
\text{s.t.} \; & \sum_{i\in\mathcal{I}_t} x_t^i = x_t & \forall t \in \mathcal{T}
\end{aligned}
$$

$$\sum_{t\in\mathcal{T}} x_t = G \qquad [\hat{u}]$$

$$0 \le x_t^i \le q_t^i - q_t^{i-1} \qquad \forall i \in \mathcal{I}_t \backslash \{1\}, \forall t \in \mathcal{T}$$

$$0 \le x_t^1 \le q_t^1 \qquad \forall t \in \mathcal{T}$$

Here $\mathcal{I}_t$ is the index set that corresponds to optimal consumption values (and their corresponding u value) in the U-C curve for each trading period $t \in \mathcal{T}$ (edge of U-C curve's steps). Note that once we have the U-C curves for each time period, solving the LP above has a trivial computational cost. When $\hat{G} \in \mathcal{G}$ the optimal consumption values in [HEU] are are also optimal for [CM-MIP]. On the other hand, when $\hat{G} \notin \mathcal{G}$ the optimal consumption values form a feasible solution to [CM-MIP]. However, [HEU]'s solution has advantages over other feasible consumption values. Suppose $\delta = \min_{G' \in \mathcal{G}}\{\hat{G} - G' \mid \hat{G} - G' > 0\}$. In other words, in [HEU], we optimize to which time period(s) the consumption quantity δ should be allocated.

When we use [HEU] to solve our model with several time periods and total consumption value $\hat{G}$, many of time periods' consumption values remain the same as the [U-MIP] model's optimal consumption values for the marginal utility value $\hat{u}$. Thus we can use the stored optimal ILR quantity value of the $[\text{U-MIP}]_{t,\hat{u}}$ model for the time periods t whose optimal consumption values remained unchanged. For those time periods t, whose optimal consumption values in [HEU] is different from that of $[\text{U-MIP}]_{t,\hat{u}}$, we solve $[\text{U-MIP}]_{t,\hat{u}}$ again but with a constraint on its consumption level, forcing it to be equal to the optimal value in [HEU], and therefore we can determine the updated optimal ILR quantity for that time period.

Note that by increasing the number of stages, the relative gap between the total consumption values in $\mathcal{G}$ decreases, which results in a lower relative optimality gap. In the next section we present bounds on gaps between the optimal solution and the heuristic policy.

3.5 Bounds

In order to demonstrate how close the optimal solution to the proposed heuristic solution is, we present upper and lower bounds on the optimal solution of [CM-MIP] (denoted by $\mathcal{Z}(G)$). When $G_i \le \hat{G} \le G_{i+1}$, and $G_i, G_{i+1} \in \mathcal{G}$, we have $\mathcal{Z}(G_i) \le \mathcal{Z}(\hat{G}) \le \mathcal{Z}(G_{i+1})$. Without loss of generality we assume that $G_2 \le \hat{G} \le G_3$, and $\mathcal{G} = \{G_1, G_2, \ldots, G_5\}$. Therefore the maximum optimality gap (for the problem with $G = \hat{G}$) is equal to $(\mathcal{Z}(G_3) - \mathcal{Z}(G_2))$. The red box in Figure 3 shows the proposed bounds in this case.

Given the structure of this problem, no better bounds can be derived without problem specific information (prices and tranche widths etc.). The quality of these bounds depends on how

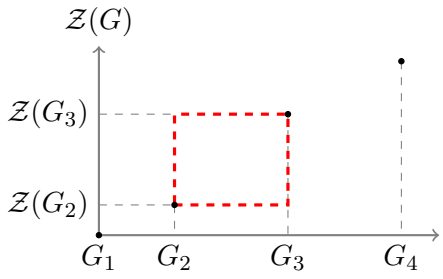

Figure 3: Cost curve

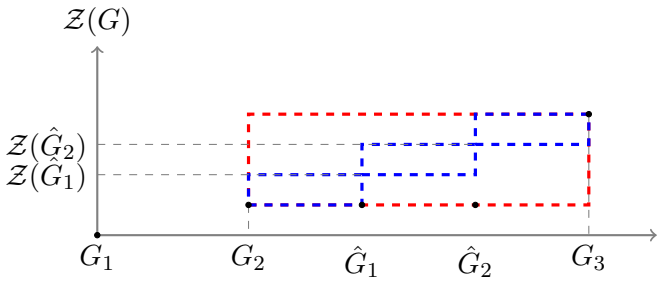

Figure 4: Cost curve - bounded

small the gaps are between the total consumption quantities. When the time periods are not identical, the increase in number of time periods can lead to smaller gaps. In the case that the time horizon includes several identical time periods, the gaps can stay large, but by using the heuristics method we can find optimal solution in between the gaps ($\mathcal{Z}(\hat{G}_1)$ and $\mathcal{Z}(\hat{G}_2)$ in Figure 4). In the following corollary we prove that any solution of [HEU] in which each $x_t = \sum_{i \in \mathcal{I}_t} x_t^i$ is equal to a q_t in the corresponding time period (a *vertex solution*), is an optimal solution to our original cost minimizing problem.

Corollary 3.2.1. *Any optimal vertex solution to [HEU] is an optimal solution to [CM-MIP].*

Proof. Any optimal vertex solution to [HEU] yields a total consumption value $G := \sum_{t \in \mathcal{T}} x_t^*$. Lemma 3.1 then establishes the result that $\mathbf{x}^*$ solves [CM-MIP]. □

This means that if the total consumption quantity $\hat{G}$ is not in $\mathcal{G}$ and it is used as the total consumption parameter in [HEU] and returns a vertex solution, then this solution solves [CM-MIP]. Furthermore, from Corollary 3.2.1, we have that there exists an ordered set $\mathcal{G}' = \{G_1, G_2, ..., G_m\}$ whereby [HEU] returns a vertex solution. Now, we know that the maximum gap between any pair of total consumption values in $\mathcal{G}'$ is the maximum consumption in one time period ($G_{i+1} - G_i \leq \max\{q_j\}$). Hence for large total consumption values (e.g. for optimization over long time-horizons), the size of this approximation, as a percentage of the total consumption, becomes insignificant. We can put the steps developed above together in an algorithm to produce a (near) optimal consumption schedule for the large consumer of interest.

Deterministic U-C algorithm: DUCA

1. **Construct individual TP U-C curves** $g(u,t)$

   Solve $[\text{MIP}]_{t,u}$ to find $\mathbf{x}_t = \mathbf{x}_t^*$ set $g(u,t) = x_t^*, \quad \forall u \in [0, u_{\max}],\ \forall t \in \mathcal{T}$.
2. **Make the aggregated U-C curve** $G(u)$

   $G(u) = \sum_{t \in \mathcal{T}} g(u,t), \quad \forall u \in [0, u_{\max}]$.
3. **For a given total consumption value** $\hat{G}$**, find a corresponding** u **value**

   If $\exists \hat{u} \in [0, u_{\max}]$ where $G(\hat{u}) = \hat{G}$:

– **Directly use $\hat{u}$ value to determine optimal consumption values at each TP**

$\hat{x}_t = g(\hat{u}, t), \quad \forall t \in \mathcal{T}.$

Else:

– **Use the heuristic model to determine consumption values at each TP**

Solve [HEU] with $G = \hat{G}$. If x_t^* is the optimal consumption values of [HEU] $\rightarrow \hat{x}_t = x_t^* \quad \forall t \in \mathcal{T}$.

4. **Return consumption values and corresponding ILR quantities**[4]

For each time period return $\hat{\mathbf{x}}_t$.

Note that the construction methodology for our aggregate U-C curve ensures that in step 3 of the algorithm above, we choose an optimal, or near optimal consumption level. In subsection 4.2 we generalize this to the stochastic expected aggregated U-C curves construction algorithms. In addition, in subsection 4.4 we lay out our stochastic U-C policy implementation algorithm.

3.6 Multistage co-optimization example

In order to demonstrate the impact of multistage co-optimization we lay out an example over a 3-node network. The 3-node network's configuration is laid out in Appendix B. In this example, we build a multistage model which is solved over twelve time periods, where the time horizon starts with off-peak time periods, then it transitions to shoulder (i.e. medium consumption), peak and again shoulder trading periods, respectively. We assume that the difference in time periods is only in the inelastic demand and the reserve requirement, while the energy and reserve offer stacks are identical in all time periods. (See Appendix B for offer stack data).

We assume that the major consumer is required to consume a total of 240 MWh of electricity over the time horizon. In order to probe the impacts of co-optimization of energy and reserve we present two versions of our model, first, we consider a major consumer who chooses its consumption quantity, and has the ability to offer ILR. Secondly, a major consumer who only decides on its consumption level and cannot offer ILR; we call these two versions v1 and v2, respectively. Utilizing our decomposition method, we build the individual trading period U-C curves, and subsequently, the aggregated U-C curves for v1 and v2 (Figure 5). Utilizing the U-C curves above, we can derive the U-C policy as well as the heuristic method that was presented in Section 3.4. In Table 1 we lay out the consumption level values of our proposed policies for both v1 and v2. Note that the solution of normal U-C policy is to over-consume energy;

[4]The optimal ILR quantity is computed simultaneously with the optimal consumption value for each u at time period t. These values can be stored to be used in this step of the algorithm.

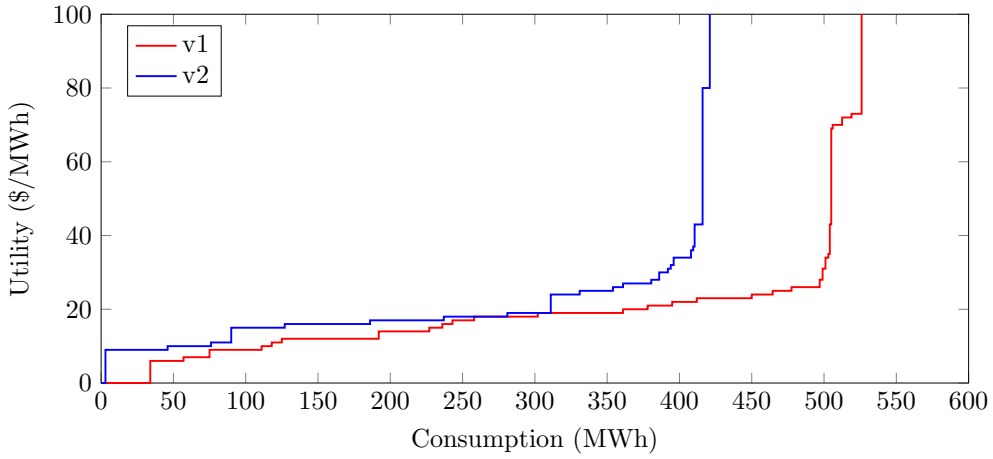

Figure 5: Aggregated U-C curves for v1 and v2

the heuristic policy however, aims to consume the exact amount of energy throughout the time horizon (the instances when quantities differ between the two policies are highlighted in red).

		Time Period												
		1	2	3	4	5	6	7	8	9	10	11	12	Total
U-C	v1	17	19	16	29	25	24	10	9	9	29	25	31	243
Heu	v1	17	16	16	29	25	24	10	9	9	29	25	31	240
U-C	v2	39	34	16	29	25	24	2	3	2	29	25	31	259
Heu	v2	17	34	19	29	25	24	2	3	2	29	25	31	240

Table 1: Consumption levels for normal U-C vs heuristic policy

Policy	v1	v2
Heuristic	2617.6	3494.5
Optimal	2604.1	3476.5

Table 2: Total cost ($)

From the policies that are presented in Table 1, we can observe that in peak time periods (7–9), the strategic consumer's demand is higher in v1 compared to v2. This is because in v1 with higher consumption levels the strategic consumer, capable of offering ILR, can offer more ILR and take advantage of high reserve prices at peak periods. But, in v2 in peak prices the consumer reduces its consumption; this leads to more consumption in off-peak periods.

In Figure 6 we depict the realized energy and reserve prices for v1 and v2, that are derived from the heuristic U-C policy. In addition, we compare our consumption policies with a fixed policy. We report on the fixed consumption policy, in which the strategic agent consumes 20MWh at each trading period (and co-optimizes ILR, similar to v1). In Figure 6, we also demonstrate the realized energy prices of the fixed consumption model for v1 at each trading period.

As shown in Figure 6, compared to the fixed consumption policy, our U-C policies prevent high energy prices at peak time periods (7–9), and consume more at off-peak trading periods (1–3). In addition, reserve prices in v2 are never less than v1, meaning that offering ILR by the

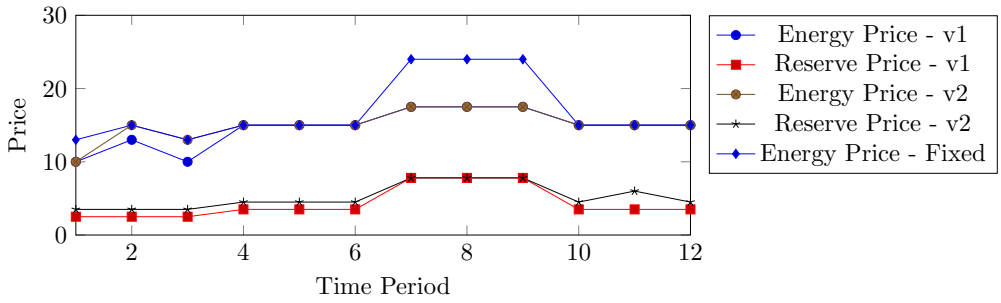

Figure 6: Energy and reserve prices in v1 and v2

consumer may lower reserve prices. In order to further compare our policy's performance we compare the results with the optimal solution that is derived from directly solving [CM-MIP] for v1 and v2. In Table 2, we present the total cost of implementing each presented policy.

4 Stochastic co-optimization over a time horizon

In this section we transition to a stochastic version of [MIP]. Our goal is to utilize the models developed here for real world applications, hence it is imperative that we account for future uncertainty at the planning stage. In order to facilitate mathematical exposition, in this section we define a scenario tree [11] and index variables by their corresponding node in the tree. We use the following notation in the rest of this section:

- $\mathcal{N}$ is the set of all nodes in the scenario tree;
- $\mathcal{N}_t$ is the set of nodes in time period t;
- x_n is the electricity consumption at node n of the tree;
- $\mathbf{x}_n$ is the vector of actions at node n of the tree;
- $\mathcal{C}_n$ is the cost function at node n;
- $\mathcal{S}_n$ is the feasible set of actions at node n;
- u_n is the u parameter corresponding to node n;
- $\mathbf{P}_m$ is the vector of nodes that form the path that terminates at leaf node m;
- ρ_n is the probability of reaching node n (via any path); and
- $\rho_{n,l}$ is the probability of reaching node l from node n in the tree.

Similar to the deterministic case, we seek to minimize expected total cost of consumption over the time horizon. We denote this stochastic problem [S-MIP]; this optimization problem seeks to minimize expected cost over all paths of the scenario tree as given below:

$$\begin{aligned} \text{[S-MIP]} \quad & \min \sum_{t\in\mathcal{T}} \sum_{n\in\mathcal{N}_t} \rho_n \mathcal{C}_n(\mathbf{x}_n) \\ & \text{s.t. } \mathbf{x}_n \in \mathcal{S}_n \qquad\qquad \forall n \in \mathcal{N}_t, \forall t \in \mathcal{T} \end{aligned}$$

$$\sum_{n \in \mathbf{P}_m} x_n = G \qquad \forall m \in \mathcal{N}_T$$

We can extend the decomposition methodology of the deterministic case here, but here we will first decompose by scenario (much like [20]), then by time.

In order to implement the optimal consumption strategy, the stochastic and non-anticipative nature of the scenario tree must be respected. We will therefore need suitably aggregated U-C curves that encode this information. To do so, we are guided by the principle that the optimal value of consumption in each period is precisely the quantity that will yield a marginal cost of consumption now, equal to the expected marginal cost of consumption in the future, at least in convex cases. We illustrate this principle initially on the convex problem that captures the price taker consumer's planning problem.

Recall the price-taking consumer from Section 3.2.1, now in a multistage setting, formulated as a stochastic dynamic program, and in absence of any integrality requirements. In $[\text{D-LP}]_t^n$ defined below, at each stage, the linear program minimizes cost, with total consumption to go (g_t) as the state variable. By the assumption that the expected future in the last time period $t = T$ is zero ($C_{T+1}^l(g_{T+1}^n) = 0$), for period t and any scenario tree node $n \in \mathcal{N}_t$ we have:

$$\begin{aligned} [\text{D-LP}]_t^n \quad C_t^n(g_t) = \min\ & \mathcal{C}(\mathbf{x}_t^n) + \sum_{l \in \mathcal{N}^{t+1}} \rho_{n,l} C_{t+1}^l(g_{t+1}^n) \\ \text{s.t. } & x_t^n + g_{t+1}^n = g_t. \qquad [u_t^n] \end{aligned}$$

Theorem 4.1. *Consider u_t^n, the dual on the consumption constraint at stage t defined in [D-LP]$_t^n$. Then*

$$\sum_{l \in \mathcal{N}^{t+1}} \rho_{n,l} \frac{\partial C_{t+1}^l(g_{t+1}^n)}{\partial g_{t+1}^n} = u_t^n, \text{ and } \quad \frac{\partial \mathcal{C}(\mathbf{x}_t^n)}{\partial x_t^n} = u_t^n.$$

Proof. Simply apply optimality conditions to $[\text{D-LP}]_t^n$ to obtain the above. □

The equations above show that u_t^n can be used to control the optimality condition, which indicates that at each node of the tree the marginal cost equals to marginal cost-to-go. In the next part, we use this property, to define the marginal utility vs. marginal cost relationship in the price maker model. This approach is explained in detail in section 4.2, but prior to that we make a short detour to deal with the discrete nature of the optimal consumption quantities.

4.1 Price-making consumer

In the price maker stochastic model, as well as the deterministic version, we are faced with the problem of corner point solutions. Here, the decomposed model's optimal solution is only

equivalent to that of the original problem for a set of discrete total consumption levels, where there exist a different set for each path $m \in \mathcal{N}_T$. In order to address this issue, we introduce [S-MIP-ϵ^+], where $\epsilon_m^+ \geq 0$ is added to the total consumption on each path. We will focus attention on [S-MIP-ϵ^+], instead; although [S-MIP-ϵ^+] is not exactly equivalent to [S-MIP], the deviation of its optimal solution from that of [S-MIP] is small enough for the purposes of our model (large total consumption value over a long time-horizon).

$$\begin{aligned}
[\text{S-MIP-}\epsilon^+] \quad \min \ & \sum_{t\in\mathcal{T}} \sum_{n\in\mathcal{N}_t} \rho_n \mathcal{C}_n(\mathbf{x}_n) & \\
\text{s.t.} \ & \sum_{n\in\mathbf{P}_m} x_n = G + \epsilon_m^+ & \forall m \in \mathcal{N}_T \\
& \mathbf{x}_n \in \mathcal{S}_n & \forall n \in \mathcal{N}_t, \forall t \in \mathcal{T}.
\end{aligned}$$

The next step is to use Lagrangian methods to decompose [S-MIP-ϵ^+]. We define $[\text{L-MIP}]_\mu$, where μ is the vector of Lagrangian multipliers (μ_m is the Lagrange multiplier on path m's total consumption constraint). Furthermore, in the objective function of $[\text{L-MIP}]_\mu$, the total consumption constraint corresponding to each path m is weighted with the probability of occurrence of path m (ρ_m). Note that $[\text{L-MIP}]_{\mathbf{x},\mu}$ is decomposable by time-period.

$$\begin{aligned}
[\text{L-MIP}]_\mu \quad \min \ & L(\mathbf{x},\mu) = \sum_{n\in\mathcal{N}} \rho_n \mathcal{C}_n(\mathbf{x}_n) - \sum_{m\in\mathcal{N}_T} \sum_{n\in\mathbf{P}_m} \rho_m \mu_m x_n + \sum_{m\in\mathcal{N}_T} \sum_{n\in\mathbf{P}_m} \rho_m \mu_m (G + \epsilon_m^+) & \\
\text{s.t.} \ & \mathbf{x}_n \in \mathcal{S}_n & \forall n \in \mathcal{N}.
\end{aligned}$$

Here, the last term in the objective function is constant and will therefore not impact the optimal consumption values. If we solve $[\text{L-MIP}]_\mu \ \forall \mu_m \in (0, \mu_m^{\max})$, we obtain a set of corresponding total consumption values for each path m, hence we can find the smallest total consumption $\hat{G}_m$, where $\hat{G}_m = G + \epsilon_m^+, \ \epsilon_m^+ \geq 0$. Here, $\hat{G}_m$, and therefore ϵ_m^+ are functions of μ_m. Note that the structure of our model for each path guarantees that $\epsilon_m^+ < C$, where C is the maximum consumption at one time period (as shown for the deterministic case in Section 3.5).

Lemma 4.2. *Let* $\mathbf{x}^*$ *be the vector of optimal consumption values of* $[\text{L-MIP}]_{\mu^*}$ *such that* $\sum_{n\in\mathbf{P}_m} x_n^* := G + \epsilon_m^+$ *and* $\epsilon_m^+ \geq 0$. *Then* $\mathbf{x}^*$ *solves* [S-MIP-ϵ^+].

Proof. Using the Lagrangian sufficiency theorem (presented in Appendix D) we prove that $\mathbf{x}^*$ is optimal for [S-MIP-ϵ^+]. First, note that the feasible regions of both problems are identical. Hence $\mathbf{x}^*$ is a feasible solution of [S-MIP-ϵ^+] and $L(\mathbf{x}^*, \mu^*) \leq L(\hat{\mathbf{x}}, \mu^*), \ \forall \hat{\mathbf{x}} \mid \hat{\mathbf{x}}_n \in \mathcal{S}_n$. □

In the next step we calculate the expected value of u parameter (that is used in the aggregated U-C curve), based on indexing the problem by paths, whereby we have:

$$\sum_{n\in\mathcal{N}} \rho_n u_n^* x_n^* = \sum_{t\in\mathcal{T}} \sum_{n\in\mathcal{N}_t} \rho_n u_n^* x_n^* = \sum_{m\in\mathcal{N}_T} \sum_{n\in\mathbf{P}_m} \rho_m \mu_m x_n^*. \tag{4.1}$$

Hence we can calculate the optimal marginal utilities, u_n^*, that meet (4.1).

$$\sum_{n\in\mathcal{N}} \rho_n u_n^* x_n^* = \sum_m \sum_{n\in\mathbf{P}_m} \rho_m \mu_m x_n^* = \sum_{n\in\mathcal{N}} \sum_{m|n\in\mathbf{P}_m} \rho_m \mu_m x_n^* = \sum_{n\in\mathcal{N}} x_n^* \sum_{m|n\in\mathbf{P}_m} \rho_m \mu_m$$

$$\implies \sum_{n\in\mathcal{N}} u_n^* x_n^* \Big(\sum_{m|n\in\mathbf{P}_m} \rho_m \Big) = \sum_{n\in\mathcal{N}} x_n^* \Big(\sum_{m|n\in\mathbf{P}_m} \rho_m \mu_m \Big)$$

$$\implies u_n^* = \frac{\sum_{m|n\in\mathbf{P}_m} \rho_m \mu_m}{\sum_{m|n\in\mathbf{P}_m} \rho_m}$$

Note that the above calculation can be performed recursively starting from the leaf nodes. In the next subsection, we will lay out the construction of the expected U-C curves with an algorithm based on the equation above.

4.2 Stochastic U-C curves

We denote by $u_n(q)$, the marginal value of electricity consumption at level q, at the tree node n (note that u is a set valued map and for some qs there is an interval of corresponding marginal costs u). Similarly, we define the function $g(u, n)$ which indicates the consumption value (q) at node n, with marginal utility u. As discussed above, in order to make the optimal choice of consumption in a given period, we must know the expected cost of future consumption. Clearly, this must be reflected through a single (expected aggregated) U-C curve, as we can not anticipate the future.

In our proposed method, we model the uncertainty in our SDP as a time in-homogeneous Markovian process. In order to model the stage-wise dependency, we use the transition probabilities. We use notation $\rho_{n,l}$ to show the probability of transitioning from node n to node l in the tree[5]. In addition, we define an artificial node $\hat{n}$ for stage zero as $\mathcal{N}_0 = \{\hat{n}\}$, where $\rho_{\hat{n},l}$ is the probability of being at node l at stage one. We use these transition probabilities to construct the U-C curves with conditional expectation.

In order to build the stochastic U-C curves, we start by building the expected curve for the last trading period ($t = T$) that is observed by each node $n \in \mathcal{N}_{T-1}$; this is constructed by assigning $\sum_{l\in\mathcal{N}_T} \rho_{n,l} u_l(q)$ to quantity q (see Figure 7). This step is referred to as "vertical expectation", and the resulting curve as expected cost to go curve.

By stepping backward, for each node $n \in \mathcal{N}_t$ in the current stage ($t = T-1$), we are in a position to map out the marginal cost of consumption for any quantity q by assessing the cheaper of the two options, namely consume now or leave it for the future. This process will naturally deliver updated U-C curves for each node in the current period as depicted in Figure 8. We label this

[5]In Section 4.5 we will show how we calculate the transition matrix, for our price-making consumer model.

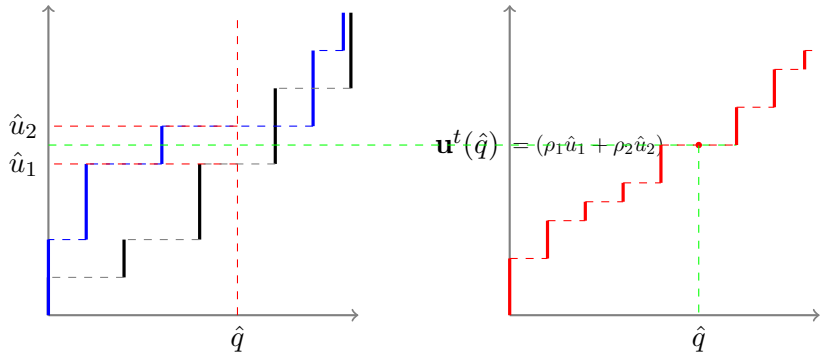

Figure 7: Vertical expectation step of constructing aggregated expected U-C curves

procedure "the horizontal aggregation". Once the updated curves of all nodes of stage t are available, we proceed to the vertical expectation step, which results in the expected cost to go curve for $n \in \mathcal{N}_{t-1}$. We do this recursively as outlined in the SUC-construction algorithm below. At the end of the algorithm, we are equipped with a look up table for optimal consumption at each node of the tree.

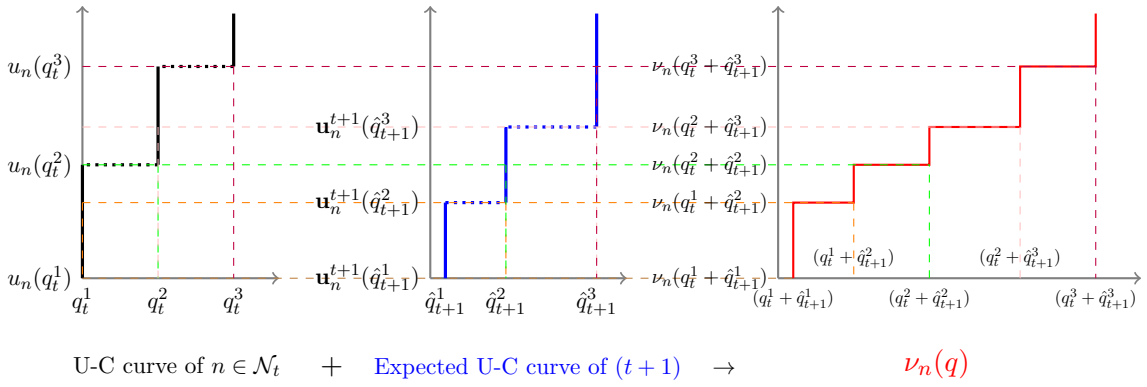

Figure 8: Horizontal aggregation step of constructing aggregated expected U-C curves

Given the step-wise form of the U-C curves, we can implement the above procedures in a relatively computationally inexpensive manner, by first acquiring the set of q values at the edge of each step. We can find the corresponding u values for all q levels between two consecutive edges. Let Ξ_n denote the set of all consumption values that shape the vertical steps in the U-C curve of node n. We also define the set of optimal (corner point) consumption-to-go values at node n as $\mathcal{Q}_n$ (for $t = T$, $\mathcal{Q}_n = \Xi_n$). We denote the set of optimal consumption-to-go values at stage t by $\mathcal{Q}^t = \bigcup_{n\in\mathcal{N}_t} \mathcal{Q}_n$. We sum up this method by **SUC-construction** algorithm below:

1. Set $t = T$.
2. $\forall n \in \mathcal{N}_{t-1}$: $\mathbf{u}_n^t(q) = \sum_{m\in\mathcal{N}_t} \rho_{n,m} u_m(q), \quad \forall q \in \mathcal{Q}^t$ (Figure 7).
3. $t \longrightarrow t-1$.

4. $\forall n \in \mathcal{N}_t$: $\mathcal{K}_n = \{(q_t, \hat{q}_{t+1}) | u_n(q_t) = \mathbf{u}_n^{t+1}(\hat{q}_{t+1}), \forall q_t \in \Xi_n \cup \mathcal{Q}^{t+1}\}$ (Figure 8).

   $\mathcal{Q}_n = \{q | q = q_t + \hat{q}_{t+1}, \forall (q_t, \hat{q}_{t+1}) \in \mathcal{K}_n\}$.
5. $\forall n \in \mathcal{N}_t$: $\nu_n(q) = u_n(q_t) | q = q_t + \hat{q}_{t+1}, \forall (q_t, \hat{q}_{t+1}) \in \mathcal{K}_n$ (Figure 8).
6. $\forall n \in \mathcal{N}_{t-1}$: $\mathbf{u}_n^t(q) = \sum_{m \in \mathcal{N}_t} \rho_{n,m} \nu_m, \quad \forall q \in \mathcal{Q}^t$ (Figure 7).
7. If $t > 1$, go to step 3. If $t = 1$, $\mathbf{u}_n^t$ is the function corresponding to the aggregated expected U-C curve in node n, at stage one.

4.3 Heuristics

In the stochastic setting, we can use a similar model to the heuristic algorithm that we proposed in the deterministic model in order to solve the [S-U-MIP] problem for any given $\hat{G}$. Similar to the deterministic model, here, at each stage of solving the dynamic programming we are faced with two curves. One is the current time-period's utility-demand curve and the other one is the curve corresponding to the expected future. Therefore we define [S-HEU] as below:

$$
\begin{aligned}
\text{[S-HEU]} \quad \min \quad & \sum_{n \in \{\text{Now,Future}\}} \sum_{i \in \mathcal{I}_n} u_n^i x_n^i & & \\
\text{s.t.} \quad & \sum_{n \in \{\text{Now,Future}\}} \sum_{i \in \mathcal{I}_n} x_n^i = \hat{G} & & [\hat{u}] \\
& 0 \le x_{\text{Now}}^i \le q^i - q^{i-1} & \forall i \in \mathcal{I}_{\text{Now}}/\{1\} \quad & (q^i, q^{i-1} \in \Xi_n) \\
& 0 \le x_{\text{Future}}^i \le q^i - q^{i-1} & \forall i \in \mathcal{I}_{Future}/\{1\} \quad & (q^i, q^{i-1} \in \mathcal{Q}^{t+1})
\end{aligned}
$$

In [S-HEU] the index "Now" refers to the current node $n \in \mathcal{N}_t$ of the scenario tree (which is in the current stage t), therefore $\mathcal{I}_{\text{Now}}$ denotes the indexes of the set of u values that correspond to the optimal consumption levels in the U-C curve corresponding to node $n \in \mathcal{N}_t$ ($u_n(q), \forall q \in \Xi_n$). Similarly, the index "Future" refers to the expected future as is observed by the current node in the tree. Hence $\mathcal{I}_{\text{Future}}$ denotes the indexes for the set of u values that correspond to all optimal (corner point) future consumption-to-go values that are observed by node n ($\mathbf{u}_n^{t+1}(q), \forall q \in \mathcal{Q}^{t+1}$). The optimal consumption values in [S-HEU] form a feasible solution to [S-CM-MIP]. The optimal solution to [S-HEU] solution has advantages over other solutions.

4.4 Stochastic U-C policy implementation

Here we lay out the algorithm that we use to obtain near optimal policies with utilization of U-C curves, when given a total consumption value $\hat{G}$ over the time horizon $\mathcal{T} = \{1, 2, \ldots, T\}$.

Stochastic U-C algorithm: SUCA

1. **Construct the aggregated expected U-C curve from subsection 4.2**
   Calculate $v_n(q), \forall q \in \mathcal{Q}_n, \forall n \in \mathcal{N}_t, \forall t \in \mathcal{T}$.

2. **Start forward pass**. Set t = 1 and set consumption to go $G = \hat{G}$.
3. **For the realized node of tree $n \in \mathcal{N}_t$, find the corresponding u value**
   If $G \in \mathcal{Q}_n$:
   - **Directly use $\nu_n(G)$ to determine optimal consumption value**[6] **at stage t** $\hat{x}_t = g(\nu_n(G), n)$.

   Else:
   - **Use the heuristic model to determine the consumption value at stage t**

     Solve [S-HEU] with $G = \hat{G}$. Given x^*_{Now} is the optimal consumption value of [HEU] for present stage $\rightarrow \hat{x}_t = x^*_{\text{Now}}$.
4. **Update consumption to go value in the forward pass**. Set $G = G - \hat{x}_t$.
   If $t \neq T$:
   - **Go to next step**. Set $t = t + 1$ and go to step 3.

   Else:
   - **End of simulation**

4.5 Modelling uncertainty

In this section we address scenario sampling methods, scenario trees and the structure of uncertainty. The section is divided into two parts, firstly, we present a tailor-made clustering method in order to address the uncertainty within our model's endogenous pricing process. Secondly, we probe different types of uncertainty and their impact on the scenario tree layout.

4.5.1 Scenario clusters

The size of a multistage stochastic program's scenario tree increases exponentially with the number of scenarios that are included in each stage, and the length of the time horizon. Thus, the large-scale models that are of interest to us, may well become computationally intractable. One of the methods used to tackle this curse of dimensionality is to utilize scenario clustering techniques to reduce the size of the scenario tree [1,4,5,7,11,12]. In most of the sample-processing methods that are used for the multistage models, the stochastic process is the representative of a stochastic exogenous parameter over the time-horizon [2,3,10,13,14]. For instance, stochastic processes for demand or price are most commonly used in electricity market models, where the exogenous electricity prices or demand levels are approximated through representative scenarios along the time horizon. However, in our model, given the price-making nature of the agent of interest, the possible future scenarios cannot be properly approximated by a few exogenous parameters. Hence the accuracy of a parametric stochastic process would not be sufficient.

[6] The optimal ILR quantity is computed simultaneously with the optimal consumption value for each node n and for each u value. These values can be stored to be used in this step of the algorithm.

In order to construct a price process that adequately represents the future, we only focus on the impacts of the uncertainty in the market participant's actions on the strategic node. The parameters within each scenario impact our model's objective function through the energy and reserve prices at the strategic node; these prices are functions of the consumer's actions as well as those of other market participants (generators and other consumers). Given this endogenous nature of the strategic node's prices, the information that we need from each scenario is the strategic node's energy and reserve price for all possible actions of the strategic consumer. We take a price sensitivity analysis approach to define representative scenarios. Without loss of generality, and in order to reduce the number of scenario clusters, we only consider energy prices to be of importance in our clustering method.

In this section, Ω_t denotes the set of all outcomes (scenarios) restricted to stage t. In effect this is similar to $\mathcal{N}_t$, where each $n \in \mathcal{N}_t$ corresponds to a scenario $\omega \in \Omega_t$. Let $\pi_t^\omega(l)$, denote the energy price that is the outcome of solving the OPF model for scenario ω and stage t, with the strategic consumption level $l \in \mathcal{L}$. In order to further quantify our sensitivity analysis, we first define the price ranges and assign an index (r) to each price range (p_r). Table 3 presents an example of possible price ranges for our model.

r	1	2	3	4	5
p_r	0-20	20-40	40-60	60-100	$\geq$100

Table 3: Price ranges

At the next step we assign the price range indices to each consumption level (l). Therefore, we denote the cluster of scenario ω at stage t ($\mathbf{c}_t^\omega$), as a vector with $|\mathcal{L}|$ elements, where $(\mathbf{c}_t^\omega)_l = r|\pi_t^\omega(l) \in p_r$. Defining scenarios by vectors enables us to utilize the idea of representative scenarios. Therefore, given that each unique vector represents a cluster, scenarios that result in the same vector of price-ranges can be considered to be in the same cluster.

In addition to defining the clusters, we must calculate the relative frequency of each cluster occurring for each type of time period. This can be done through counting the number of members of each cluster over the sample space. Using these clusters we can also address stage-wise dependence in the price process as markov process. We can estimate a transition matrix based on transition frequencies. Utilizing the resulting transition matrix alongside with the method described in subsection 4.2, we can construct the expected U-C curves over a designated time horizon. (See Appendix E for NZAS's tailor-made scenario clusters and the corresponding transition matrix for our case study.)

4.5.2 Scenario realizations

In this part we discuss different structures of uncertainty for our mathematical model. So far we used a wait-and-see approach in defining our model where, at each stage, the realized scenario is known, even though all future stages' scenarios that would be realized are uncertain. Depending on the nature of uncertainty, we may wish to lay out our model with a here-and-now decision process. In this setting, we know which scenario ω is realized only after we make a decision. In order to capture such uncertainty, at each stage, t, we need to solve a MIP equivalent of a stochastic bi-level problem for the strategic consumer, for which the optimal consumption maximizes the expected profit over a set of scenarios for that stage (Ω_t). In Appendix C, we have laid out the stochastic bi-level optimization problem, that then is reformulated as a MIP, which we refer to as [H-MIP]$_{t,u}$. We solve the stochastic [H-MIP]$_{t,u}$, $\forall t \in \mathcal{T}$, which maximizes expected profit (with marginal utility value of u) over $\omega \in \Omega_t$ where Ω_t is the set of possible future scenarios for stage t.

Although wait-and-see or here-and-now methods are useful in modelling specific types of stochasticity, in practice, decision making under uncertainty is a combination of wait-and-see and here-and-now actions, given the difference in our ability of predicting different uncertain parameters. Therefore, we combine the here-and-now and wait-and-see approaches into a hybrid method, in order to present a more realistic stochastic process.

We first utilize the type of uncertainty that cannot be accurately predicted to make scenarios for [H-MIP]$_{t,u}$. In the case of our model, such uncertainties arise from real-time fluctuations in demand or wind. In addition, we incorporate the wait-and-see uncertainty that follow known patterns and can be anticipated, to build the set of states in each stage of the scenario tree for the stochastic model [S-MIP]. Such uncertainties are built into our model as the estimated generation offers, as well as average demand and prices, depending on the time-of-day, day-of-week and season of a trading period.

For our stochastic optimization model, the hybrid scenario tree illustrates our implementation of scenario clusters, where each node in the scenario tree represents a unique type of time period, which we refer to as a cluster. Each cluster consists of scenarios that share similar patterns of generation offers and total demand. Given that market participants have a good estimate of the type of trading period they are in (in terms of generation offers and total demand), before making their decision, we define clusters in a wait-and-see setting. On the other hand, the real-time fluctuations of the market need to be addressed through a here-and-now stochastic model, within each cluster. (See Appendix F for a detailed implementation of the hybrid method for

NZAS.) In the next section we utilize our hybrid method in our case study of a large consumer in New Zealand.

5 Case study

In this section, we implement our stochastic model for the New Zealand aluminum smelter (NZAS), an industrial consumer of energy in the NZEM. The strategic consumer's load is large enough to affect the energy price at its node. Also, it is capable of offering ILR, and can thereby influence the reserve price within the South Island of New Zealand. We solve our model for a given total consumption level to determine our consumption policy over a time-horizon based on our proposed method. The expected cost of this policy is compared to the operating policy of NZAS which consumes a fixed volume over all trading periods.

Utilizing **SUCA** algorithm (from subsection 4.4), we simulate our stochastic U-C policy with out-of-sample paths. (See Appendix G for a detailed NZAS out-of-sample policy simulation implementation.) In order to present a detailed report on the policy performance, we limit our example to analysis of one season, winter. Hence, we construct our sample space using historical data from winters 2016–2018. Our proposed algorithm for solving stochastic multistage demand-response allows us to solve our model over a time-horizon of up to one month in a reasonable time-frame. In this section, we report on the average cost of 200 different sample paths. We present numerical results for short-term (daily), mid-term (weekly) and long-term (monthly) demand scheduling.

5.1 Daily scheduling

In this section we simulate our daily consumption policies using random sample paths and compare it with a fixed policy, in which the consumption rate stays the same throughout the time horizon. Note that in order to simulate the fixed policy, we run our model for the out-of-sample scenarios with the given fixed consumption rate and compare the total cost with our policy. In our case study, the total consumption requirement for one day is set to 13728MWh[7], hence at the fixed policy, the consumption is 572MW at all time periods[8]. In Table 4, we report on the average total expected cost over 200 paths, for U-C policy and the fixed policy.

In order to further illustrate the policies' performance, we choose a random sample path and report on each stage's optimal actions. In this example, we compare our policy with a fixed policy, where the same level of consumption applies to each stage. In Figure 9 we present

[7]Note that in the NZEM trading periods are half-hours. Therefore, if the consumer's consumption rate is 100MW, during one trading period it consumes 50MWh.

[8]572MW is the fixed rate that was used by the NZAS in the historical data that we have used.

	Expected cost ($)	Average Price ($/MWh)
U-C Policy	966,225	69.8
Fixed Policy	1,166,420	85.6

Table 4: Daily scheduling comparison

a comparison between optimal actions, followed by a plot showing the realized prices in each stage, given the consumption level. This shows that our policy is able to utilize the off peak time periods and consume more, such as TP9. Furthermore, our policy adjusts the consumption in peak time periods and reduces its level in order to alleviate spike prices, TP17 is an example of such time periods, where the fixed policy results in much higher price than our policy's realized price. In order to demonstrate the difference in stage-wise dependent (the method that we use) and the stage-wise independent approach, we compare the two methods in Appendix H.

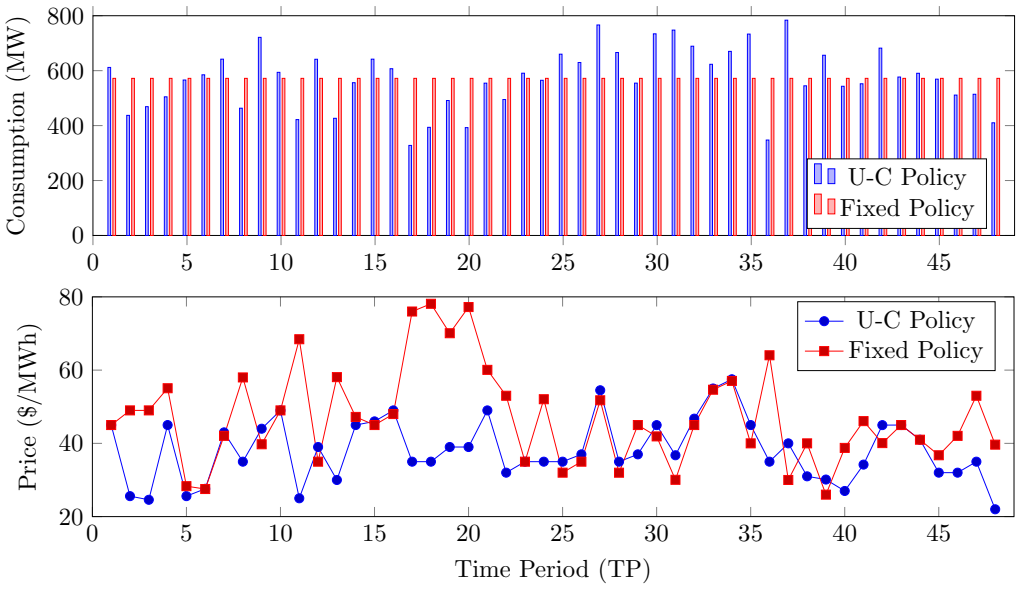

Figure 9: Policy comparison

5.2 Weekly scheduling

In this section, we simulate our proposed policy on a week-long time horizon. We first report on the performance of our method, in comparison with the fixed consumption policy. Secondly, we discuss the length of time horizon, and how the strategic consumer can decrease its total cost if it schedules demand over a longer time period. Note that in weekly scheduling simulation, the time horizon consists of $48 \times 7 = 336$ stages. The algorithm used to employ our U-C curves as the marginal value's look-up table is the same as depicted in Figure 12. Moreover, Table 5 compares the U-C and fixed policy, when simulated for 200 random sample paths. For these simulations, the total consumption (G) equals $336 \times 572 \times \frac{1}{2} = 96096$MWh.

	Expected cost ($)	Average Price ($/MWh)
U-C Policy	6,677,076	67.23
Fixed Policy	8,042,006	82.91

Table 5: Weekly scheduling comparison

The longer the time horizon for demand scheduling is, the longer it takes to construct the U-C curves. On the other hand, the extended time horizon allows us to take into account further future information in our present actions, and to have more opportunity to shift load to low price periods. In this part, we lay out an example in which we compare the performance of two policies; the first one is solving the stochastic demand scheduling problem through utilizing U-C curves, for random sample paths, over a week-long time horizon, with $G = 96096$MWh. In the second example, we use the same sample paths that we used in the first example, but here we solve a sequence of seven one-day long scheduling problems, where we set the total consumption required for each of these days' policies to be the same: $96096/7 = 13728$MWh.

Schedule		Mon	Tues	Wed	Thur	Fri	Sat	Sun
Weekly	Load (MWh)	13714	14258	12731	14014	13584	13961	13831
Daily	Load (MWh)	13728	13728	13728	13728	13728	13728	13728
Weekly	Cost ($)	864,854	1,097,349	794,562	869,550	748,289	777,241	837,680
Daily	Cost ($)	867,953	1,020,440	980,425	848,277	836,657	748,979	822,674
Weekly	Price ($/MWh)	58.7	72.9	60.2	61.1	52.4	54.3	56.6
Daily	Price ($/MWh)	59.5	71.0	68.8	60.9	58.3	53.8	56.0

Table 6: Weekly scheduling comparison

Table 6 shows the benefits of the flexibility in total consumption in one day versus one week. Here we compare the total load in one day for the two policies, while the aggregated amount for the whole week stays fixed. The results demonstrate that the weekly scheduling is more able to adjust consumption to take advantage of lower priced days more than the daily scheduling policy. The total cost in daily scheduling over the 7 days is $6,125,408 which is 2.2% higher than that of the weekly scheduling, which is $5,989,527. Moreover, the last two rows of this table show the time-weighted average price at the strategic node, under the two types of scheduling. We observe that nodal price of higher priced days (e.g. Wednesday) reduces when we are able to shift load between days in the weekly scheduling. We further illustrate the results in Figure 10, where we laying out the detailed consumption levels and prices for Wednesday and Thursday.

As shown in Figure 10, the weekly scheduling scheme reduces total consumption on Wednesday, but compensates for it in the following days. On the other hand, the daily scheduling is set to consume the fixed total consumption and therefore on Wednesday the average price becomes about $8 more than that of the weekly scheduling model. On Thursday, weekly schedule's

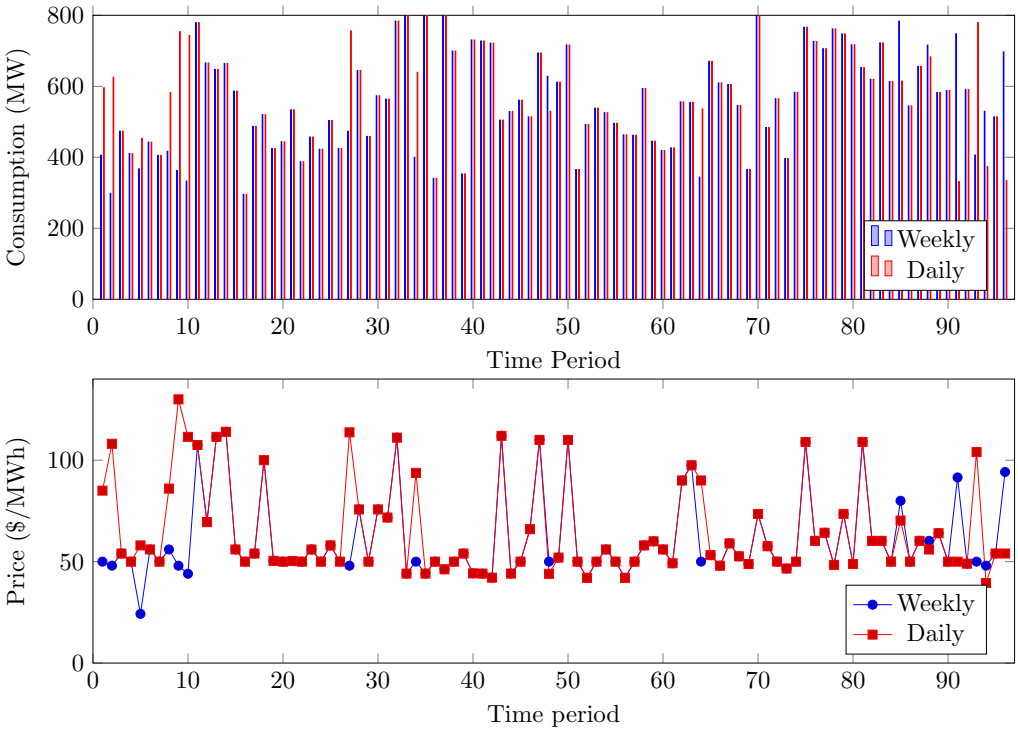

Figure 10: Weekly and daily policy comparison

total consumption (14014MWh) is more than the total amount in the daily scheduling policy (13728MWh), but the difference in the average price of energy is only 20 cents.

5.3 Monthly scheduling

The length of the period of a production plan primarily depends on the duration of the contracts with its clients. The length of a firm's manufacturing schedule, can also be affected by sustained and considerable increases or decreases in the price of its product. For instance, if a firm observes that the local or global price of its product is constantly dropping, it might want to set a lower production level for the next scheduling period. In order to practically address the contract length, and the price signals, we have chosen the duration of one month as the longest time-horizon for our case study on NZAS's demand scheduling.

In this section we present numerical results for monthly demand-scheduling with our U-C policy and compare it with a fixed consumption policy. Note that for our case study the number of trading periods in one month is $(48 \times 7 \times 4 = 1344)$. Solving a stochastic multistage program over a large time-horizon raises concerns on both the accuracy of generated policies and the practicality of implementation. The first issue is due to the unavailability of reliable information for the time-periods that are far in the future. Therefore, the parameter estimates for the scenarios at the time periods which are close to the end of a long time-horizon can become

inaccurate. However, as we approach these time periods in our forward pass, we could gain more useful information on the parameter values associated with these TPs. For instance, the weather forecast becomes more accurate as it gets closer to the date, resulting in better estimates of reservoir levels and temperature. Secondly, building the U-C curve becomes more cumbersome as the planning period becomes longer. When large number of U-C curves are aggregated, the width of the steps in the aggregated expected U-C curve become smaller, which requires larger numbers of calculations in each recursion and much larger memory space.

In order to address the accuracy and practicality issues, we propose a time-adaptive aggregation method for building U-C curves. Given that the information on future time periods evolves as we move forward in time, we build the individual U-C curves for the farther time periods with less detail. Hence, when constructing U-C curves for scenarios in distant time periods, the intervals of u values in $\{0, u_{\max}\}$ are larger than for those closer to the start of our time-horizon.

In order to implement the time-adaptive U-C curve approach for the monthly scheduling, after constructing the first aggregated expected U-C curve (at day 0), we run our forward pass, and at the end of each week, we update the aggregate U-C curve that is corresponding to the remaining weeks. Table 7 presents the interval updates at the end of each week in the forward pass.

	Day 0	Day 7	Day 14	Day 21
week 1	1	-	-	-
week 2	1	1	-	-
week 3	10	1	1	-
week 4	10	10	1	1

Table 7: Bisection search u intervals

	Exp cost ($)	Ave Price ($/MWh)
Standard U-C Policy	21,160,509	62.6
Updated U-C Policy	21,276,065	62.7
Fixed Policy	25,499,180	82.4

Table 8: Monthly scheduling comparison

In the monthly scheduling case study, we used 100 random sample paths, using the historical data for winter 2016 and 2017. In order probe the impacts of updating U-C curves, we conduct the following experiments on these 100 sample paths and report the average results. The first experiment is our standard U-C policy and assumes sufficient and consistent availability of information for all the four weeks in the horizon. In the second experiment we assume that, for each sample path, less information is available for weeks three and four at the beginning of simulation. Therefore the U-C curve is based on less detailed future data. Here, we implement the time-adaptive U-C policy, and use Table 7 to construct and update our aggregated U-C curves. Note that the same sample paths are used in these two experiments. In Table 8 we compare the updating mechanism with the standard U-C policy, and the fixed consumption method. Here, we observe that the expected cost in the updated U-C policy is only 0.5% higher than the standard U-C policy, which is an acceptable trade-off for reducing the problem size whilst also enabling the updating of future scenario distributions.

6 Conclusions

In this paper, we presented a model that solves a large-scale extended time-horizon strategic electricity consumption scheduling problem. The major consumer in this model, purchases electricity from the spot market, and is also able to offer ILR. We assumed a price-making major consumer (modeled via a MIP), who observes the impacts of its decisions on the market. In order to be able to solve such a large MIP over an extended time-horizon, we used Lagrangian methods to decompose the multistage stochastic demand and ILR co-optimization. Our method determines the consumer's optimal demand and ILR offer by adjusting the marginal value of consuming electricity to the type of trading period.

We implemented our optimization method for a large consumer of energy in New Zealand. Our policy simulation over out-of-sample scenarios showed the advantage of our proposed method, which resulted in on average 18% cost reduction compared to the fixed consumption policy. We also showed that, by extending the time-horizon, our method takes advantage of the higher flexibility in consumption level which leads to lower total cost. For instance, weekly scheduling saves about 2%, when compared to daily scheduling for the same total consumption over the seven days. By utilizing our proposed method, we also solved the multistage demand planning over one month, for NZAS, a large manufacturer in New Zealand. Our algorithm allows for incorporating stage-wise dependent scheduling, as well as updating and tuning the look-up table as the information about the future evolves in the forward pass.

Finally, we showed that the strategic behavior of a major consumer who purchases electricity from the wholesale market and has flexible load, not only decreases its own costs but also lowers the spot price of electricity, which can also benefit smaller consumers.

References

[1] P. Beraldi and M. E. Bruni. A clustering approach for scenario tree reduction: an application to a stochastic programming portfolio optimization problem. *Top*, 22(3):934–949, 2014.

[2] R. S. Dembo. Scenario optimization. *Annals of Operations Research*, 30(1):63–80, 1991.

[3] R. S. Dembo, A. Chiarri, J. G. Martin, and L. Paradinas. Managing hidroeléctrica española's hydroelectric power system. *Interfaces*, 20(1):115–135, 1990.

[4] J. Dupačová, G. Consigli, and S. W. Wallace. Scenarios for multistage stochastic programs. *Annals of operations research*, 100(1-4):25–53, 2000.

[5] J. Dupačová, N. Gröwe-Kuska, and W. Römisch. Scenario reduction in stochastic programming. *Mathematical programming*, 95(3):493–511, 2003.

[6] S. C. Graves. A review of production scheduling. *Operations research*, 29(4):646–675, 1981.

[7] N. Growe-Kuska, H. Heitsch, and W. Romisch. Scenario reduction and scenario tree construction for power management problems. In *Power tech conference proceedings, 2003 IEEE Bologna*, volume 3, pages 7–pp. IEEE, 2003.

[8] M. Habibian, A. Downward, G. Zakeri, M. F. Anjos, and M. Ferris. Co-optimization of demand response and interruptible load reserve offers for a price-making major consumer. 2017.

[9] T. Hansen, E. Chong, S. Suryanarayanan, A. Maciejewski, and H. Siegel. A partially observable Markov decision process approach to residential home energy management. *IEEE Transactions on Smart Grid*, 2016.

[10] W. Härdle. *Applied nonparametric regression*. Number 19. Cambridge university press, 1990.

[11] H. Heitsch and W. Römisch. Scenario tree modeling for multistage stochastic programs. *Mathematical Programming*, 118(2):371–406, 2009.

[12] R. Henrion, C. Küchler, and W. Römisch. Discrepancy distances and scenario reduction in twostage stochastic mixed-integer programming. *Journal of Industrial and Management Optimization to appear*, 2008.

[13] M. Hollander and D. A. Wolfe. Nonparametric statistical methods. 1999.

[14] J. Jacobs, G. Freeman, J. Grygier, D. Morton, G. Schultz, K. Staschus, and J. Stedinger. Socrates: A system for scheduling hydroelectric generation under uncertainty. *Annals of Operations Research*, 59(1):99–133, 1995.

[15] T. T. Kim and H. V. Poor. Scheduling power consumption with price uncertainty. *IEEE Transactions on Smart Grid*, 2(3):519–527, 2011.

[16] H. Luo, B. Du, G. Q. Huang, H. Chen, and X. Li. Hybrid flow shop scheduling considering machine electricity consumption cost. *International Journal of Production Economics*, 146(2):423–439, 2013.

[17] S. Misra, A. Mondal, S. Banik, M. Khatua, S. Bera, and M. S. Obaidat. Residential energy management in smart grid: a Markov decision process-based approach. In *Green Computing and Communications (GreenCom), 2013 IEEE and Internet of Things (iThings/CPSCom), IEEE International Conference on and IEEE Cyber, Physical and Social Computing*, pages 1152–1157. IEEE, 2013.

[18] S. Mitra, I. E. Grossmann, J. M. Pinto, and N. Arora. Optimal production planning under time-sensitive electricity prices for continuous power-intensive processes. *Computers & Chemical Engineering*, 38:171–184, 2012.

[19] M. Nistor and C. Antunes. Integrated management of energy resources in residential buildings: a Markovian approach. *IEEE Transactions on Smart Grid*, 2016.

[20] R. T. Rockafellar and R. J.-B. Wets. Scenarios and policy aggregation in optimization under uncertainty. *Mathematics of operations research*, 16(1):119–147, 1991.

[21] P. Samadi, H. Mohsenian-Rad, V. W. Wong, and R. Schober. Tackling the load uncertainty challenges for energy consumption scheduling in smart grid. *IEEE Transactions on Smart Grid*, 4(2):1007–1016, 2013.

[22] T. J. Scott and E. G. Read. Modelling hydro reservoir operation in a deregulated electricity market. *International Transactions in Operational Research*, 3(3-4):243–253, 1996.

[23] G. Steeger, T. Lohmann, and S. Rebennack. Strategic bidding for a price-maker hydroelectric producer: Stochastic dual dynamic programming and lagrangian relaxation. *IISE Transactions*, (just-accepted):1–28, 2018.

[24] G. Steeger and S. Rebennack. Dynamic convexification within nested benders decomposition using lagrangian relaxation: An application to the strategic bidding problem. *European Journal of Operational Research*, 257(2):669–686, 2017.

[25] Z. Sun and L. Li. Potential capability estimation for real time electricity demand response of sustainable manufacturing systems using Markov decision process. *Journal of Cleaner Production*, 65:184–193, 2014.

[26] M. P. Taylor, J. J. Chen, M. Farid, and R. J. Wallace. Heat exchanger, Mar. 8 2011. US Patent 7,901,617.

[27] Z. Yu, L. Jia, M. C. Murphy-Hoye, A. Pratt, and L. Tong. Modeling and stochastic control for home energy management. *IEEE Transactions on Smart Grid*, 4(4):2244–2255, 2013.

Appendix

A Co-optimized strategic energy bidding and interruptible load reserve offering

In this appendix we lay out a profit maximization problem that is solved by a major consumer of energy in a co-optimized energy and reserve market, where the consumer is able to offer ILR. We first present the co-optimized optimal power flow (OPF) problem over a multi-node network. We use the following notation:

f_{ij}	The flow between node i and j.
K_{ij}	The line capacity in arc ij.
r_e	The reserve level required in zone e.
V_n	The minimum amount of difference between ILR and consumption, at node n. It denotes the level of consumption that can not be interrupted.
B_n	The fraction of generation allowed to be offered at reserve, at node n.
W_n	The maximum total amount of generation and reserve, offered by the generator , at node n.
$\mathcal{N}$	The set of all nodes in the network. Note that in our model we have one agent per node. This is not a restrictive assumption.
$\mathcal{N}^*$	The set of the strategic nodes. In our model $\|\mathcal{N}^*\| = 1$
$\mathcal{A}$	The set of all arcs in the network.
$\mathcal{N}_e$	The set of all nodes in zone e.
L	The loop constraint matrix, where $L_{l,ij}$ corresponds to row l (associated with each loop) and the column ij corresponds to arc ij.
$\mathcal{T}'^n_c$	The set of interruptible consumption tranches.
e_n	indicates the zone that node n is located in.
$\mathcal{E}$	The set of zones.
$\mathcal{Z}$	The set for types of tranches, i.e. consumption, generation, ILR and reserve. $\mathcal{Z} = \{c, g, rc, rg\}$
$\mathcal{T}_z$	The set of all offered tranches of type z.
$\mathcal{T}^n_z$	The set of all tranches of type z at node n
y^z_t	The variable associated with the dispatch quantity tranche type z.
p^z_t	The price of tranche t of type z.
q^z_t	The quantity of tranche t of type z.
[ ]	Variables in [ ] indicate the duals of their associate constraints.

$$\text{[OPF]} \max_{y^c, y^g} \sum_{t_c \in \mathcal{T}_c} p^c_{t_c} y^c_{t_c} - \sum_{t_g \in \mathcal{T}_g} p^g_{t_g} y^g_{t_g} - \sum_{t_{rg} \in \mathcal{T}_{rg}} p^{rg}_{t_{rg}} y^{rg}_{t_{rg}} - \sum_{t_{rc} \in \mathcal{T}_{rc}} p^{rc}_{t_{rc}} y^{rc}_{t_{rc}}$$

$$\text{s.t.} \quad \sum_{t_c \in \mathcal{T}^n_c} y^c_{t_c} + \sum_{i|ni \in \mathcal{A}} f_{ni} - \sum_{i|in \in \mathcal{A}} f_{in} = \sum_{t_g \in \mathcal{T}^n_g} y^g_{t_g} \qquad [\pi^d_n] \qquad \text{(A.1)}$$

$$- \sum_{n \in \mathcal{N}_e} \sum_{z \in \{rc, rg\}} \sum_{t_z \in \mathcal{T}^n_z} y^z_{t_z} = -r_e \qquad [\pi^r_{e_n}] \qquad \text{(A.2)}$$

$$\sum_{ij \in \mathcal{A}} L_{l,ij} f_{ij} = 0 \qquad [\lambda_l] \qquad \text{(A.3)}$$

$$-K_{ij} \leq f_{ij} \leq K_{ij} \qquad [\eta^+_{ij}, \eta^-_{ij}] \qquad \text{(A.4)}$$

$$0 \leq y^z_{t_z} \leq q^z_{t_z} \qquad [\nu^{z+}_{t_z}, \nu^{z-}_{t_z}] \qquad \text{(A.5)}$$

$$\sum_{t_{rc} \in \mathcal{T}^n_{rc}} y^{rc}_{t_{rc}} - \sum_{t_c \in \mathcal{T'}^n_c} y^c_{t_c} \leq 0 \qquad [\theta_n] \qquad \text{(A.6)}$$

$$\sum_{t_{rg} \in \mathcal{T}^n_{rg}} y^{rg}_{t_{rg}} \leq B_n \sum_{t_g \in \mathcal{T}^n_g} y^g_{t_g} \qquad [\phi_n] \qquad \text{(A.7)}$$

$$\sum_{t_{rg} \in \mathcal{T}^n_{rg}} y^{rg}_{t_{rg}} + \sum_{t_g \in \mathcal{T}^n_g} y^g_{t_g} \leq W_n \qquad [\phi'_n]. \qquad \text{(A.8)}$$

Here (A.1), and (A.6) to (A.8) hold $\forall n \in \mathcal{N}$. (A.2) holds $\forall e \in \mathcal{E}$. (A.3) holds for each loop, indicating that sum of impedance adjusted flows across the loop must be zero. (A.4) holds $\forall ij \in \mathcal{A}$. (A.5) holds $\forall t_z \in \mathcal{T}_z, \forall z \in \mathcal{Z}$. Using the OPF model, laid out above, we formulate the bi-level optimization problem, that we call [B-L], below:

$$\text{[B-L]} \quad \max_{x_n, x^r_n} \sum_{n \in \mathcal{N}^*} \left(u x_n - \pi^d_n x_n + \pi^r_{e_n} x^r_n \right)$$

$$\text{s.t.} \quad 0 \leq x_n \leq C^d_n \qquad \text{(A.9)}$$

$$0 \leq x^r_n \leq C^r_n \qquad \text{(A.10)}$$

$$x_n - x^r_n \geq V_n \qquad \text{(A.11)}$$

$$\text{[OPF2]} \quad \max_{y^{z|z \in \mathcal{Z}}} \sum_{t_c \in \mathcal{T}_c} p^c_{t_c} y^c_{t_c} - \sum_{t_g \in \mathcal{T}_g} p^g_{t_g} y^g_{t_g} - \sum_{t_{rg} \in \mathcal{T}_{rg}} p^{rg}_{t_{rg}} y^{rg}_{t_{rg}} - \sum_{t_{rc} \in \mathcal{T}_{rc}} p^{rc}_{t_{rc}} y^{rc}_{t_{rc}}$$

$$\text{s.t.} \quad \text{(A.1)} - \text{(A.8)}$$

$$\sum_{t_c \in \mathcal{T}^n_c} y^c_{t_c} + \sum_{i|ni \in \mathcal{A}} f_{ni} - \sum_{i|in \in \mathcal{A}} f_{in} = \sum_{t_g \in \mathcal{T}^n_g} y^g_{t_g} - x_n \qquad [\pi^d_n] \qquad \text{(A.12)}$$

$$- \sum_{n \in \mathcal{N}_e} \sum_{z \in \{rc, rg\}} \sum_{t_z \in \mathcal{T}^n_z} y^z_{t_z} = x^r_{n_{|n \in \mathcal{N}_e}} - r_e \qquad [\pi^r_e]. \qquad \text{(A.13)}$$

Here we solve a slightly different OPF problem as the lower level problem which we called [OPF]. The difference is in adding the strategic consumption and ILR variables to the OPF

model. Hence here (A.9) to (A.11), and (A.12) hold $\forall n \in \mathcal{N}^*$. In addition, (A.1) holds $\forall n \in \mathcal{N} - \mathcal{N}^*$. For reserve requirement, which is met on the zonal level, if the strategic node is in zone e, (A.13) is enforced, and for all other zones, we enforce (A.2). This bi-level model is then reformulated as a MIP. (See [8], for details on the reformulation algorithm.)

B Co-optimization example's market data

In this appendix, we present the network structure, and the parameter values that are used in our 3-node example. As illustrated in Figure 11, the network contains a loop (impedance equals 1.0 for all arcs) with buses A, B and C. In this example we assume that there are two generators, one at bus B and one at bus C. We also assume there is an inelastic consumer at bus C and the strategic consumer at bus A. The line capacities are shown in Figure 11.

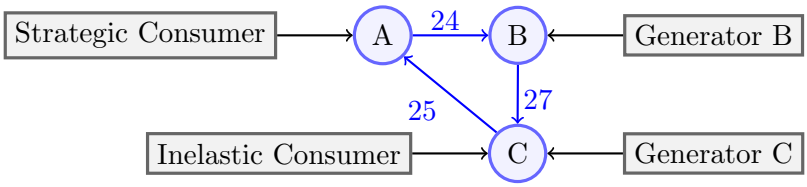

Figure 11: The 4-node network.

Table 9 presents energy and reserve offer stack data. Here, the maximum amount of aggregated reserve and energy available from generators B and C are 50 and 75 MW, respectively.

Gen B Energy		Gen C Energy		Gen B Reserve		Gen C Reserve		Cons C ILR	
quantity	price	quantity	price	quantity	price	quantity	price	quantity	price
15	9	15	10	10	2.5	13	4.5	20	300
7	13	15	15	15	3.5	15	6		
7	18	10	17.5	15	4.1	17	7.8		
8	20	9	19.2	10	6.5	17	11		
7	23	9	24	10	8.7	20	22		

Table 9: Energy and reserve offer stack data.

Moreover, Table 10 presents the values of demand and reserve parameters associated with each time period.

	Time Period											
	1	2	3	4	5	6	7	8	9	10	11	12
Bus C Inelastic Demand (MW)	13	18	14	23	27	28	52	53	53	23	27	21
Reserve Requirement (MW)	18	21	17	36	31	39	71	69	70	35	42	36

Table 10: Inelastic demand and reserve levels

C Stochastic co-optimization for a strategic major consumer

In order to address uncertainty we define a stochastic model, where the strategic consumer decides on its optimal consumption level, that would maximize expected profit over the set of scenarios Ω, where the probability of occurrence of each scenario ω is ρ^{ω}. We lay out this stochastic bi-level problem [S-B-L], as below:

$$\begin{aligned}
\text{[S-B-L]} \quad & \max_{x_n, x_n^{r^\omega}} \quad \sum_{\omega\in\Omega} \rho^{\omega} \sum_{n\in\mathcal{N}^*} \left(u x_n - \pi_n^{d^\omega} x_n + \pi_{e_n}^{r^\omega} x_n^{r^\omega} \right) \\
& \text{s.t.} \quad \text{(A.9)} - \text{(A.11)} && \forall \omega \in \Omega \\
& \qquad [\text{OPF2}]^{\omega} && \forall \omega \in \Omega
\end{aligned}$$

D Lagrangian sufficiency theorem

Theorem D.1. *If x^* and λ^* exist such that x^* is feasible for [P] and $L(x^*, \lambda^*) \leq L(x, \lambda^*) \quad \forall x \in \mathcal{X}$,then x^* is optimal for [P].*

Proof. Define

$$\mathcal{X}_b = \{x : x \in \mathcal{X} \text{ and } g(x) = b\}$$

Hence $\forall x \in \mathcal{X}_b$ we have:

$$L(x, \lambda) = f(x) - \lambda^{\top}(g(x) - b) = f(x)$$

Now $x \in \mathcal{X}_b \in \mathcal{X}$, and so by assumption:

$$f(x^*) = L(x^*, \lambda^*) \leq L(x, \lambda^*) = f(x) \qquad \forall x \in \mathcal{X}_b.$$

Which concludes, x^* is optimal for [P]. □

E Scenario clusters for NZAS

In order to build scenario clusters, we sample multiple scenarios from the sample space (winters 2016–2018) for each stage t over the time horizon $\mathcal{T}$. We distinguish the type of a stage (γ) by the trading period of the day (TP $\in \mathcal{P}$), the type of day ($d \in \mathcal{D}$), as weekend or weekday, and the season ($s \in \mathcal{S}$). Hence there exist $|\mathcal{P}| \times |\mathcal{D}| \times |\mathcal{S}|$ types of stages; we call the set of all types of stages as Γ. Depending on the length of the time horizon, the number of types of stages that are included in the model is different. For instance, in our monthly scheduling model, we target one season $|\mathcal{S}| = 1$, therefore we have ($|\Gamma| = 48 \times 2 \times 1 = 96$). Note that two stages can share the same γ (e.g. 2 p.m. in all weekdays of winter). Utilizing the above definitions, we assign a sample space $\Theta_\gamma, \forall \gamma \in \Gamma$, where each sampled scenario $\theta \in \Theta_\gamma$ is derived from the historical data of trading periods of type γ.

Moreover, $\forall \gamma \in \Gamma$, we run the vSPD (the OPF problem for the NZEM) $\forall \theta \in \Theta_\gamma$, for different designated levels of consumption $l \in \mathcal{L}$ for our strategic consumer (the NZAS in NZEM) and report on the corresponding energy prices at the strategic node (Tiwai Point). Using this method, we can determine the kind of each scenario, in terms of realized prices corresponding to different strategic consumption levels. Table 11 shows an example of the change in price by increasing consumption of the strategic consumer, for a group of sample scenarios.

Date and Time	Parameters			Load (MW)		
	s	d	TP	300	500	700
5/07/2016 0:00	w	w–d	1	21.2	41.678	49.401
5/07/2016 0:30	w	w–d	2	26.651	44.535	56.011
5/07/2016 1:00	w	w–d	3	18.289	41.697	47.902
5/07/2016 1:30	w	w–d	4	9.117	36.413	47.332
5/07/2016 2:00	w	w–d	5	4.715	34.558	46.749

Table 11: Price sensitivity analysis

In order to further quantify the sensitivity analysis, we assign an indicative value to each price range.

Utilizing Table 3's price range definitions, we assign the price range numbers to each consumption level and make Table 12. Note that we picked 5 price ranges, since it was a good trade-off

between accuracy and practicality. In Table 12, we view each row as a vector where each unique vector is a cluster. For example, the first two scenarios of this sample are in one cluster, with a corresponding cluster vector [2,3,3].

Date and Time	Parameters			Load (MW)		
	s	d	TP	300	500	700
5/07/2016 0:00	w	w–d	1	2	3	3
5/07/2016 0:30	w	w–d	2	2	3	3
5/07/2016 1:00	w	w–d	3	1	3	3
5/07/2016 1:30	w	w–d	4	1	2	3
5/07/2016 2:00	w	w–d	5	1	2	3

Table 12: Price range clusters

We derive the set of clusters $\mathbf{C}_\gamma$ through the above algorithm $\forall \gamma \in \Gamma$; here each cluster $c \in \mathbf{C}_\gamma$ consists of a subset of sample scenarios Θ_γ^c. Furthermore, $\bigcup_{c \in \mathbf{C}_\gamma} \Theta_\gamma^c = \Theta_\gamma$ and all subsets Θ_γ^c are pairwise disjoint. Using the above definitions, we integrate the notion of a hybrid scenario tree with our clusters (as described in subsection 4.5.2). In our model's scenario tree, at each stage t with type γ, we have $|\mathbf{C}_\gamma|$ nodes, and represent each node with the [H-MIP]$_{t,u}$ model (introduced in Appendix C), that is solved over the scenario set Θ_γ^c (in the next subsection we will use the solution of [H-MIP]$_{t,u}$ to build the corresponding U-C curves). In addition to defining the clusters, we calculate the probability distribution of the clusters (c) at each type of stage γ (as illustrated in subsection 4.5.1) and denote it by φ_γ^c.

F Expected U-C curves for NZAS

In order to construct the expected U-C curve over the time horizon $\mathcal{T}$ for our case study, we first need to calculate the individual U-C curves[9] for each $t \in \mathcal{T}$. Thereafter, for our hybrid model, each individual U-C curve corresponding to stage t (where t is of type γ), and cluster c is calculated through iteratively solving [H-MIP]$_{t,u}$ over set of scenarios Θ_γ^c, which is the stochastic optimization program corresponding to cluster c.

[9]We calculate individual U-C curves as described in Section 3.3, but, instead of solving [MIP]$_{t,u}$, we solve [H-MIP]$_{t,u}$. We use a bisection search to determine the optimal consumption corresponding to marginal utility values in $\{0, u^{\max}\}$, where $\Delta u = 1$ MW is the smallest interval for u values.

When solving our multistage model, we focus on which stage ($t \in \mathcal{T}$) we are at instead of which type of stage we are facing. Therefore, we use the function $\psi(t) = \gamma$ that returns the type of stage t and update our notation as follows; we assign a scenario set Ω_t to each stage t, which consists of all clusters $c \in \mathbf{C}_{\psi(t)}$. Therefore, each cluster $c \in \mathbf{C}_{\psi(t)}$ corresponds to one scenario $\omega \in \Omega_t$; in other words, we can view each $\omega \in \Omega_t$ as the representative scenario of its corresponding cluster $c \in \mathbf{C}_{\psi(t)}$. Moreover, the probability of occurrence of $\omega \in \Omega_t$ in a stage-wise independent setting (ρ_t^{ω}) is equal to that of its corresponding cluster ($\varphi_{\psi(t)}^{c}$). Similarly, when we assume stage-wise dependency for the transition probabilities, we have: $\rho_t^{\sigma,\omega} = \varphi_{\psi(t)}^{b,c}$, where σ is the realized scenario at stage $t-1$. Note that for trading periods that are transitioning from a weekday to weekend and vice versa we set the sample set accordingly in order to maintain the information on transition probabilities. In this case study, for each trading period $t \in \mathcal{T}$, our sample space consists of 50 trading periods of type $\psi(t)$. Note that the number of clusters for each t is different.

By utilizing the method described in subsection 4.2, we construct the expected U-C curves over the designated time horizon. Here we use $\rho_t^{\sigma,\omega}$ to address the probability of transitioning from scenario σ at stage $t-1$ to ω at stage t. Note that $\rho_t^{\sigma,\omega}$ is equivalent to ρ_n, l which is the probability of going from node $n \in \mathcal{N}_{t-1}$ in the tree to node $l \in \mathcal{N}_t$ in the tree, where n and l are the tree nodes that correspond to σ and ω, respectively.

The expected U-C curve provides us with a comprehensive look-up table, thereafter, when given a total consumption G over time horizon $\mathcal{T}$, we can derive a near-optimal action from the expected U-C curve.

G Out-of-sample policy simulation algorithm

In this appendix we use the algorithm that was laid in subsection 4.4 (**SUCA**) to simulate our proposed policy. In order to address the fluctuations in demand and intermittent generation resources, we conduct an out-of-sample simulation in which we take up on a hybrid stochastic scheme where we assume that, before decision making, the type (cluster) of the realized scenario is known (wait-and-see), but the details of the particular scenario is realized after decision making (here-and-now). To simulate out-of-sample scenarios for our policy, we first build a random sample path. $\forall t \neq 1$, given $\hat{\sigma}$ is the picked scenario at $t-1$, we randomly choose scenario $\hat{\omega}_t$ from Ω_t, with probability $\rho_t^{\hat{\omega}_t}$.

Using this sample path (denoted by $\hat{\Omega}$), for each stage t, we have a randomly picked cluster

($c \in \mathbf{C}_{\psi(t)}$) that corresponds to $\hat{\omega}_t$. Thereafter, given $\hat{\omega}_t$, we can use an *out-of-sample* scenario ϖ_t, that belongs to the cluster c (corresponding to $\hat{\omega}_t$), as the realized scenario at stage t. Therefore in our forward pass, we employ an action that is extracted from the U-C curves, and apply it to the out-of-sample scenarios. Figure 12 lays out the steps of our simulation algorithm. Here the blue boxes demonstrate the exogenous setting of each simulation, in addition gray arrows are used to show the stages needed for the calculation of cost for out-of-sample scenarios.

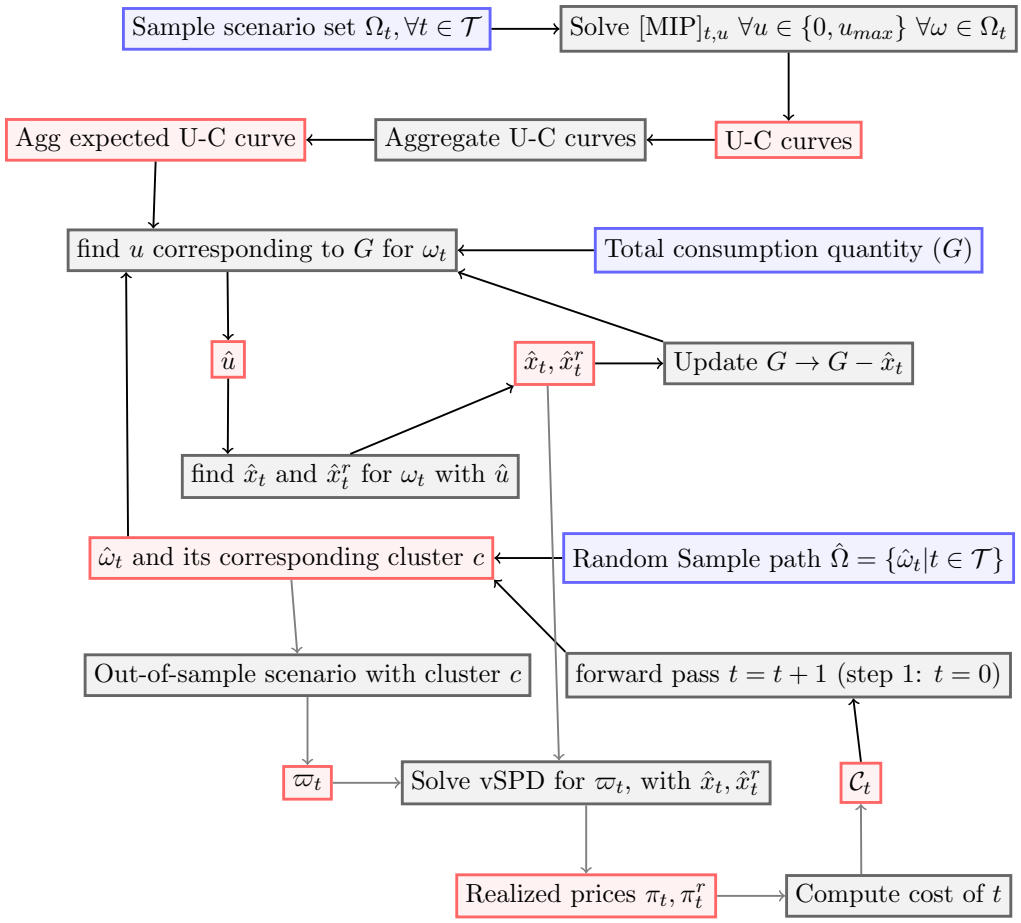

Figure 12: Optimal stochastic policy out-of-sample simulation algorithm

H Stage-wise dependency and independency

Electricity prices are affected by changes in temperature, rainfall, or in the event of generators' or transmission's shutdowns. Generally, fluctuations of electricity prices that are caused by natural phenomenons continue for a few hours. Therefore, the beginning of an unforeseen rise or fall of the price, could be used as a signal for adjusting the agent's actions in the trading periods that follow it. We address this property in our stage-wise dependent model. In this section, we present an example, that illustrates the advantages of using a stage-wise dependent

model. In this example we used a sample path that consists of scenarios with potentially higher than average prices. (Such sample path could be representative of a very cold winter day.) We simulate both our stage-wise dependent and independent U-C policies on one such sample path and report on the optimal consumption levels and realized prices for all trading periods over that day in Figure 13.

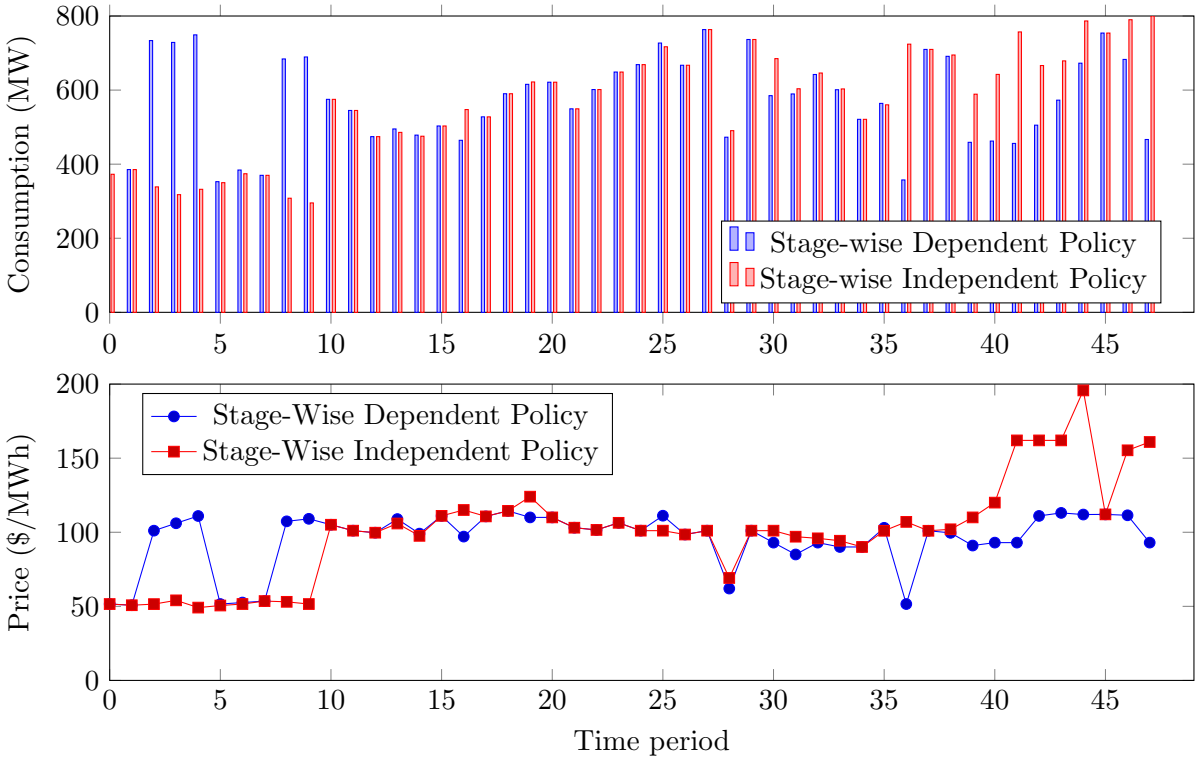

Figure 13: Stage-wise dependent/independent policy comparison

As shown in Figure 13, the stage-wise dependent policy anticipates the prospect of persisting high prices whereas, in the stage-wise independent model, the probability of lower priced scenarios in the future is high enough for the consumer to delay its consumption to later time periods in the day; this leads to very high prices towards the end of the time horizon for the stage-wise independent model.

	Expected cost ($)	Average Price ($/MWh)
U-C Policy[D]	966,225	69.8
U-C Policy[I]	1,045,437	72.1
Fixed Policy	1,166,420	85.6

Table 13: Daily Scheduling Comparison

From Table 13 we observe that the stage-wise dependent optimal policy yields the lowest average

cost over our simulations. Note that we have used the same set of (out-of-sample) sample paths for all three types of policies; in addition, our sample paths are generated using the transition probability that is described in Appendix F. The stage-wise independent model still has an advantage over the simple fixed policy, where the average nodal price for the NZAS has decreased by $13.5.